IEEE Access
Multidisciplinary | Rapid Review | Open Access Journal

Received 17 June 2022, accepted 12 July 2022, date of publication 21 July 2022, date of current version 11 August 2022.

Digital Object Identifier 10.1109/ACCESS.2022.3192971

SURVEY

Physical Layer Enhancement for Next-Generation Railway Communication Systems

QIANRUI LI[1], (Member, IEEE), JEAN-CHRISTOPHE SIBEL[1], MARION BERBINEAU[2], (Member, IEEE), IYAD DAYOUB[3,4,5], (Senior Member, IEEE), FRANÇOIS GALLÉE[6], AND HERVÉ BONNEVILLE[1]

[1]Mitsubishi Electric Research and Development Centre Europe (MERCE), 35708 Rennes, France
[2]Département Composants et Systèmes (COSYS), Université Gustave Eiffel, 59650 Villeneuve d'Ascq, France
[3]Université Polytechnique Hauts-de-France, 59313 Valenciennes, France
[4]Université Polytechnique Hauts-de-France, CNRS, University of Lille, ISEN, Centrale Lille, UMR 8520, Institut d'Électronique de Microélectronique et de Nanotechnologie (IEMN), 59313 Valenciennes, France
[5]INSA Hauts-de-France, 59313 Valenciennes, France
[6]IMT Atlantique, Lab-STICC, UMR CNRS 6285, 29238 Brest, France

Corresponding author: Qianrui Li (q.li@fr.merce.mee.com)

This work was supported by Agence Nationale de la Recherche through the mmW4Rail project under Grant ANR-20-CE22-0011.

ABSTRACT This paper presents an overview of the challenges and state-of-the-art physical layer enhancement designs for next-generation railway communication, also known as high-speed train (HST) communication. The physical layer design for HST must be adapted from its general network counterpart due to the harsh propagation environment and extreme conditions, the strict latency and reliability requirements of specialized rail applications, and the scarcity of the frequency band due to regulation. In this survey, we examine how conventional multiple-input-multiple-output (MIMO) family techniques such as beamforming, multi-cell MIMO, and relays can enhance the physical layer performance for HST. Physical layer enhancement assisted by novel reconfigurable intelligent surface (RIS) technology is also analyzed from different perspectives. Dedicated control channels, reference signals, waveforms, and numerology designs for train-to-infrastructure (T2I) and train-to-train (T2T) communication in sidelinks are also reviewed. Finally, a brief introduction to artificial intelligence (AI)/machine learning (ML)-aided HST physical layer design is provided. Several promising research avenues have also been suggested.

INDEX TERMS Railway communication, high-speed train, physical layer, MIMO, relays, reference signal, reconfigurable intelligent surface, artificial intelligence, machine learning.

I. INTRODUCTION

Enhancement and support for vertical applications and emerging use cases are among the main features of the 3rd Generation Partnership Project (3GPP) 5G New Radio (NR) specification evolution from release 15 to release 18. Owing to the harsh radio propagation environment and the distinct requirements of dedicated railway applications, conventional network deployment and physical layer design, which are dedicated to the general-purpose network should be carefully revisited to adapt to extreme communication conditions and stringent service requirements in specific use cases.

The associate editor coordinating the review of this manuscript and approving it for publication was Shuihua Wang.

Among all, the HST scenario, known as a vital use case for the future Intelligent Transport System (ITS), has attracted wide attention over the years. Within Europe, Global System for Mobiles–Railways (GSM-R), which is part of the European Telecommunications Standards Institute (ETSI)/3GPP GSM specifications with dedicated Quality of Service (QoS) requirements for a harmonized railway operation, is combined with the General Packet Radio Service (GPRS) to form the basis for an Intelligent Transport System that allows railways to improve its operation efficiency and offer new services to users. The European Rail Traffic Management System (ERTMS) is the rail management system which combines the European Train Control System (ETCS) with GSM-R. As a unique European train control system, ERTMS

is designed to gradually replace the existing incompatible systems throughout Europe. Beyond Europe, GSM-R is adopted by 56 countries for their Rail operation. The Rail Industry Group has indicated that GSM-R products and services support are guaranteed until 2030 at least. Based on this information, the railway sector must mitigate the risk of GSM-R's non-availability for train operation after this date. In Europe, the International railway union (UIC) has launched the Future Railway Mobile Communication System (FRMCS) project with the support of the European Union Agency for Railways (EUAR) to let railway operators specify the requirements for a next-generation railway communication standard. In July 2015, a new ETSI group was launched as ETSI Technical Committee on Railway Telecommunications (ETSI TC-RT). Joint Undertaking (JU) Shift2Rail also has participated in the evolution of the future train communication system. In the meantime, the investigation on the HST is at its height with such a scenario being identified in 5G as a representative use case to target consistent passenger user experience and critical train communication reliability with very high mobility [1]. Apart from industries and standardization bodies, many works have been conducted in the last decade in the academic domain as well. Previous tutorials and surveys in [2]–[6] have made excellent investigations on the challenges, feasibility, opportunities, concrete case studies, and realistic implementation issues in the HST. However, these works dated back to early 2018, when the 5G discussion was still focused on the basic features of enhanced Mobile Broadband (eMBB) and Ultra-Reliable Low Latency Communication (URLLC) for the general-purpose network. Since then, dedicated applications and requirements for railway communication have been better analyzed in UIC and 3GPP. In addition, 5G evolution has been made in release 16 and release 17 (to be finalized shortly) with enhancements such as high mobility, high-frequency band Reference Signal (RS) design, and high mobility beam management. MIMO enhancement to support multiple Transmission and Reception Points (multi-TRPs) for the Single Frequency Network (SFN) HST scenario has also been included in release 17. Therefore, it is now high time to revisit the challenges and difficulties encountered for the HST physical layer design and present an overview of the existing technologies which can serve as countermeasures.

A. CHALLENGES OF HST

In the context of climate change, the HST is now a convenient alternative for travel worldwide with the development of high-speed lines between cities. High speed, full automation, massive network capacity, and high quality of services can be achieved owing to efficient wireless systems being able to fulfill stringent requirements in terms of safety and security. However, the deployment of such a telecommunication system remains challenging because of the following specific features of HST communication.

1) HARSH ENVIRONMENT AND EXTREME CONDITIONS

In HST communication, there are very specific propagation environment scenarios such as ballast, cutting, tunnel, and viaduct. These environments are not expected in the traditional railway or automotive domains. They can create specific radio propagation phenomena such as multiple reflections and scattering on obstacles along the tracks and masking effects, which drastically impact the signal behavior [7]. For example, in a tunnel environment, the capacity of a MIMO system can be affected by the possible existence of the *Key Hole* effect [8] and spatial correlation [9]. In the case of a new type of tunnel built for very high-speed trains such as the hyper-loop train, a specific challenge, in addition to the very high speed, is how to cope with the small distance between the tunnel walls and the train. For other environments such as ballast, some authors have already highlighted their influences on millimeter-wave (mmWave) systems [10].

In addition to harsh propagation conditions and diverse environmental scenarios, HST communication also suffers from extreme conditions such as high voltage near antennas, dust, rain, snow, and vibrations of trains. The first example related to a high voltage near the antennas is the impulsive noise measured on GSM-R antennas as a consequence of electric arcs generated by bad sliding contact between the catenary and the pantograph because of wear effect or loosening of the catenary [11]. This noise can be modelled using a long-tail alpha-stable distribution [12]. In addition, in the mmWave band, the effect of train vibrations was highlighted in [13].

Interference from multiple sources is another feature that leads to difficulties in HST communication. The interference from other communication systems particularly in the ITS band has been highlighted in [14]. Jamming from other illegal anonymous communications networks is a real threat highlighted in the EU SECRET project [15]. Several solutions were proposed in [16], [17].

2) HIGH MOBILITY, HIGH FREQUENCY, AND DEDICATED REQUIREMENTS

Apart from the difficulties linked to the external environment and conditions, there are other challenges related to intrinsic HST behaviors and stringent requirements of dedicated railway applications.

First, a high Doppler shift exists owing to the high mobility of the train. In the HST scenario, the trains can reach a maximum velocity of approximately 500 km/h, which results in a severe Doppler effect in communication.

In addition, high-frequency bands, such as the FR2 band in 5G, have been considered in HST communications to solve the problem of spectrum scarcity. It is well known that high-frequency signals are subject to high path loss, blockage effect, and high penetration loss. The high-frequency band also contributes to hardware impairment. For example, phase noise is a synchronization impairment that stems from local oscillators. Even though an improvement in hardware is an

obvious solution, it is not sufficient because of the strong constraints on the radio frequency (RF) components [18].

Finally, there are various dedicated railway applications with stringent requirements for T2I and T2T communication in HST. In the framework of the FRMCS project, the UIC worked on different services that would be necessary for next-generation train [19], [20]. They divided services into three groups: critical, performance, and business. The critical group includes automatic train protection (ATP), automatic train operation (ATO), multi-party voice, virtual coupling, and critical real-time video. In the latter, there are several purposes such as video, lidar, or radar data that may be automatically processed, for example, for automated reaction to hazards in GoA3/GoA4 train operation modes. The performance group includes public address and messaging services, on-train and infrastructure telemetry, on-train remote equipment control, or non-critical video (on-board monitoring, camera helping maneuver at stations, etc.), while wireless Internet for passengers would typically be in the business group. Based on the requirements of the UIC and the railway stakeholders, 3GPP proposed in [21] a set of different traffic classes that the communication system must support in order to be able to respond to railway services. At high speeds, transmit delays shall remain below 100 ms in many cases, and shall even stay below 10 ms typically in shunting areas (low speed). In addition to the transmission delay, one salient metric when addressing critical communication is the requested reliability, that is, the percentage of packets transmitted successfully relative to the total number of packets transmitted, which could be 99.9999 % for critical data communication. The delivery guarantee of the communication system is one of the main differentiating points when addressing a critical service such as train control/command, compared to the requirement of a public communication service. Indeed, when the ETSI RT group studied 5G NR radio performance in rail environments [22], one performance metric of the simulation outputs was the 5-percentile of throughput at the worst location (typically the cell edge). This was compared with the typical metrics used when addressing public operator services, where throughput performance is typically averaged over an entire cell.

3) FREQUENCY BAND REGULATION AND COEXISTENCE

A spectrum is a shared resource by definition and is a necessary asset for any communication system. In Europe, two 4 MHz bands have been allocated to railways in the $800-900$ MHz band, dedicated to the European train control-command system GSM-R. For its upcoming successor, FRMCS, two 5.6 MHz bands were secured in the $800-900$ MHz band, and an additional 10 MHz band can be used in the 1900 MHz band [23]. Some short bands are available at 5.9 GHz but are mainly reserved for urban rail and partially shared with road ITS users. These spectral bands could be sufficient for basic control command services. However, HST development comes with new services, such as video monitoring, video for remote driving, automatic driving, virtual coupling, and maintenance data. These new requirements will push for spectrum efficiency, and a look at the exploration of mmWave frequency is essential. Another option is spectrum sharing with public communication operators, at least for non-critical services. The slicing feature facilitates this operation.

FRMCS is based on multiple radio access technologies (Wi-Fi, long-term evolution LTE, 5G, and satellite) to ensure flexibility and availability. Simultaneously, the automotive industry is working on technical solutions for connected vehicles. The ITS-G5 system has been standardized for several years, and solutions to allow hybridization with cellular systems such as LTE-Vehicle-to-everything (LTE-V2X) or Cellular-V2X (C-V2X) and future 5G NR technology are under development. In this context, the cohabitation of rail and road systems in the ITS band is important in the context of spectrum scarcity. The scenarios for the coexistence of the rail and road systems were analyzed in the public Deliverable D6.1 from the ongoing 5GRail project [24]. The possibility of sharing telecommunication infrastructure in various representative scenarios will be analyzed in the future [25].

B. SCOPE AND ORGANIZATION OF THE PAPER

In this paper, we provide a comprehensive overview of state-of-the-art HST communication physical layer design. We first introduce the challenges and difficulties linked to the harsh communication environment in HST, followed by different sections describing in detail both mature and emerging technologies for HST physical layer enhancement. These technologies have either already played a key role in the current HST physical layer design or are widely recognized as a potential paradigm shift for future system.

In Section II, we summarize how MIMO family technologies can enhance the physical layer performance of HST communication. We begin with conventional multi-user MIMO and beamforming, and then move to more sophisticated multi-transceiver and multi-cell cooperation schemes as well as relay assistance. In Section III, we introduce the novel RIS technology and demonstrate how it can lead to a better physical layer design in six aspects. In Section IV, the reference signal and waveform designs that help to defeat the specific phenomena in the HST are surveyed. In Section V, the focus is on recent advances in artificial intelligence and machine learning for the physical layer, revealing their potential in HST-related physical layer design.

II. PHYSICAL LAYER ENHANCEMENT FOR HST: MIMO AND MORE

Since the seminal work of Telatar [26], the MIMO paradigm, which equips transceivers with multiples antennas and separates simultaneous multi-user communications via their spatial signatures to achieve increased diversity and multiplexing gains, has brought numerous successes to the current wireless communication systems. It is widely used in systems with the sub-6 GHz band as well as the mmWave band in 5G NR. Owing to the rich multi-path environment

and the possibility of compact antenna array packaging in the mmWave band, several spatial streams can be exploited to improve the bit rates. In HST scenarios, MIMO also plays a pivotal role in physical layer enhancement to fight against the rapidly varying fading environment, manage the sophisticated interference regime, and improve the robustness of wireless links in next-generation railway communication systems.

A. BEAMFORMING TECHNIQUES

Beamforming techniques allow focusing on the radiation direction to improve radio link power reception and mitigate interference. When the path loss is low, full digital beamforming is possible using an elementary antenna with an omnidirectional or quasi-omnidirectional radiation pattern. In this case, the main challenge is the digital processing speed versus the fast variation in the HST propagation environment. To reduce the power consumption and cost of high-band mixed-signal components, there is a smaller number of RF chains compared to the number of antennas at the transceiver side. This type of implementation is not a new feature of the 5G NR. Dating back from LTE full-dimension MIMO (FD-MIMO), 3D beamforming in both vertical (elevation) and horizontal (azimuth) directions has already been proposed for 2D structured antenna arrays. The mapping between RF chains and antenna elements is called transmit-receive unit (TXRU) virtualization in 3GPP terminology.

In 5G FR1 (up to 7 GHz) and FR2 (mmWave band), path loss is more important. To ensure radio link quality with a minimum bit rate, a directive antenna should be used. Hence, instead of direct processing on TX and RX antennas in the conventional MIMO scheme, processing is based on TX and RX beams. In FR1, full digital beamforming is always possible but in the FR2 frequency band, hybrid analog and digital beamforming are used. The goal is to find the best compromise between antenna directivity, number of discrete beams to cover an angular sector, beamforming type (beam steering or multiple beams), and hardware complexity. The drawback of the beam-steering approach is channel uncertainty outside the main beam during communication. In the case of radio link disruption, there is no anticipation of such an event, and time is required to determine the new beam direction. By using a multi-beam antenna, the channel propagation over a large angular zone can be analyzed simultaneously during the communication. The main objective is to avoid communication interruption by radio link anticipation. The complexity of the hardware depends on the number of requested beams and the frequency. Several solutions have been proposed using reflectarrays [27] or transmit array antenna [28]–[30].

Beamforming is extremely challenging when one or both endpoints are mobile. The limitation of codebook-based beamforming in the case of mobility is as follows: if there is a significant change in the client's location, the current beam pattern is rendered useless, and a new beam has to be established towards the new location of the client. The railway environments and constraints mentioned in section I-A will drastically impact the design and optimization of codebooks for both T2I and T2T communication systems. In the literature, there are some works on codebook-based beamforming for mmWave communications in the case of high-speed trains, for example, [31]–[34]. In [31], the authors proposed two transmit diversity schemes for high-mobility massive MIMO communications with angle-domain Doppler compensation in uplink transmission for T2I communications. In [32], a ray-tracing tool was considered to obtain the spatial and temporal characteristics of the T2I propagation channel along a high-speed railway line with a specific antenna model to optimize the codebook design. In [33], using the same ray-tracing tool used in [32], standardized codebooks were considered to optimize the number of mmWave base stations along the tracks for high-data-rate T2I communications. The results were consolidated using actual tests. In [34], the HST wireless communication system design benefitted from the proposed beamforming scheme. It should be noted that location information plays a paramount role in this scheme, where the leverage among beamwidth, directivity, and how to maximize directivity under diverse positioning accuracies to guarantee efficient transmission is crucial, especially in the engineering design of HST wireless communication systems. Other open points for research in the case of high mobility were addressed in [35].

The enhancement of the carrying capacity of high-speed railways and the acceleration of train speed led to the proliferation of signal interference in the communication network, which in turn led to the degradation of network performance and user service quality. [36] proposes an algorithm that fully considers the mobility of high-speed train users and effectively manages interference. This algorithm significantly improves the performance of high-speed railway wireless communication networks. In addition, crossline trains, as a link between high-speed and conventional rail networks, increase the complexity of transport organizations and lead to significant challenges in dispatch coordination between the two systems. Based on the characteristics of high-speed transport organization, [37] dealt with the necessity of dispatch coordination between high-speed and conventional lines from the following two perspectives: the operation of crossline trains and work coordination in connection stations. An adjustment model for the operation of high-speed trains, considering crossline trains was established. Finally, the dispatch system was described in terms of its construction and process. Methods for organizing dispatch were proposed, and the processes of coordination adjustment under normal and unexpected situations were analyzed. The discussion in this paper may serve as a theoretical basis for the development of high-speed rail dispatch systems.

B. MULTI-CELL COOPERATIVE TRANSMISSION TECHNIQUES

The MIMO cooperation between multiple cells is another interesting technique for HST. This can improve spectrum efficiency and provide better interference mitigation. While

conventional MIMO techniques can greatly improve the co-channel link performances and mitigate intra-cell interference, they can hardly contribute to improving the performance of users who suffer from inter-cell interference. A conventional method for treating inter-cell interference is frequency reuse. Advanced frequency reuse methods including fractional frequency reuse and soft frequency reuse, were proposed in the standard [38]. The basic idea of frequency reuse is as follows: adjacent cells will be assigned different frequency resources such that strong inter-cell interference from close cells is prevented. However, this results in a small frequency reuse factor and inefficient spectrum management in the system. It should be noted that interference and spectrum scarcity are the two major problems in HST. Interference deteriorates the link capacity, which results in limited spectrum efficiency and transmission error. Since HST scenarios involve public safety applications that require ultra-high reliability and low latency, interference mitigation is important.

Multi-cell cooperative transmission provides a new perspective on inter-cell interference. According to different levels of cooperation and information sharing, multi-cell cooperative transmission can be categorized into three techniques: (1) interference coordination, (2) coherent joint transmission coordinated multi-point (CJT-CoMP), also known as MIMO cooperation, network MIMO, or virtual MIMO; and (3) rate-limited CoMP. Multi-cell MIMO cooperation for general-purpose networks has already been extensively studied in the literature, and an excellent survey can be found here [39]. In the following, we present MIMO cooperation between multiple cells in the HST according to the three techniques mentioned above.

1) INTERFERENCE COORDINATION

In an interference coordination scheme, a targeted cell serve only users in the cell. Nevertheless, users in other cells experience interference from the target cell. By virtue of channel state information (CSI) sharing for both direct communication links and interference links between base stations (BSs), they can coordinate their physical layer design strategies, such as beamforming, power allocation, user scheduling, and radio resource allocation to provide better multi-cell performance.

In the HST, an optimal multi-cell coordinated beamforming strategy for downlink communication was proposed in [40]. In this study, a targeted train is served by a conventional hexagonal cell BS close to the rail track. The train receives interference signals from adjacent hexagonal cell BSs. The train is considered to be an ordinary UE. The only difference from other UEs is that they have much higher mobility, which introduces additional interference caused by the Doppler effect. A coordinated beamforming strategy is proposed to maximize the data rate of the train while guaranteeing the minimal required data rates for other low-mobility users in both the serving cells and neighboring cells. In [41], coordinated power allocation for HST scenarios with multiple trains served by multiple high altitude platforms (HAPs, i.e., airborne BS) was formulated into a multi-objective optimization problem to maximize the sum rate of each HAP system. A comparison was made for different beamforming strategies, such as maximum ratio transmission (MRT), zero-forcing (ZF) beamforming, and maximal signal to leakage and noise ratio (SLNR) beamforming, under different train location conditions. In [42], a coordinated beamforming and power allocation scheme that considered a hybrid beamforming architecture with a mixed analog-to-digital converter (ADC) was investigated. The per-user achievable rate with the maximum ratio combining (MRC) receiver was derived. The coordinated power allocation optimization to maximize the per-cell sum rate under a fixed power budget was solved using a successive approximation algorithm. Although the work in [42] is not dedicated to an HST scenario, it is particularly interesting because mmWave band deployment for HST with hybrid beamforming is also envisaged for next-generation railway systems. Considering a radio access network (RAN) sharing scenario between the public safety LTE (PS-LTE) system and LTE-Railway (LTE-R) system, the work in [43] exhibits a coordinated scheduling scheme to mitigate the inter-cell interference from PS-LTE eNBs to the LTE-R network.

2) CJT-CoMP

In CJT-CoMP transmission, owing to both CSI and user data sharing, multiple cooperating nodes jointly create a large MIMO system where larger spatial diversity can be achieved. In this scenario, the multi-cell MIMO transmission returns to a virtual single-cell multi-user MIMO case. The theoretical bounds and practical precoding schemes for the equivalent broadcast channel and its dual counterpart (i.e., the multiple access channel) have been thoroughly investigated in the literature [39].

CJT-CoMP transmission has attracted special attention for HST. In 5G release 17, MIMO enhancement that targets multiple transmit and receive points (multi-TRPs) transmission for HST SFN has been standardized. In this scenario, multiple TRPs transmit the same data signal to the train, which is the CJT-CoMP transmission. For a multi-TRP transmission in an HST SFN, both a common reference signal shared among multi-TRPs and TRP-specific reference signals at different TRPs are possible. In addition to TRP-specific reference signals, release 17 supports the association of different reference signals with different channel properties. The Doppler shift and delay spread can be associated with different reference signals through a quasi-co-location (QCL) and transmission configuration indication (TCI) framework. In release 17, different QCL enhancements were studied to better support advanced channel estimation schemes that can be implemented at the train. QCL enhancements were investigated to evaluate the need for TRP-side pre-compensation algorithms [44].

3) RATE-LIMITED CoMP

In rate-limited CoMP, the backhaul link between each pair of cooperating nodes is non-ideal with a limited capacity. In 3GPP, a typical example of rate-limited CoMP is non-coherent joint transmission (NCJT) multi-TRP transmission. In this scheme, the cooperative TRPs can transmit independent streams to the target UE. Therefore, limited or no data sharing is required. In addition, full CSI sharing or no CSI sharing is needed, depending on the centralized or distributed scheduler implementation on multi-TRPs. Hence, the NCJT multi-TRP transmission is flexible for non-ideal backhaul. Owing to the limited backhaul feature, rate-limited CoMP often leads to distributed cooperation and team decision problems, which are further discussed in Section V-B3.

C. RELAY ASSISTED TECHNIQUES

Another MIMO cooperation strategy envisaged in the HST is relay. By introducing an intermediate node between the TX and RX, the relay node can communicate with both ends and mitigate the previously detrimental propagation conditions from the TX to the RX. The benefits of relay-assisted techniques are twofold [39]: they can (1) improve the effective direct channel gain between the TX and potentially remote RX and (2) mitigate the interferences via multi-node cooperation.

1) MOBILE RELAY

Most of the recent works on relay-based architecture in HST are prone to the 5G HST scenario in 3GPP. In the 5G NR study item on scenarios and requirements [1], the HST scenario with a train speed of up to 500km/h is a candidate for eMBB application in 3GPP [45]. Fig. 1 depicts the HST deployment architecture for both the FR1 and FR2 bands proposed in 3GPP [1]. In the deployment, two types of radio nodes are possibly used: dedicated linear macrocell deployment of a remote radio head (RRH) along the rail tracks and relay at the top of the train carriage. It should be noted that this

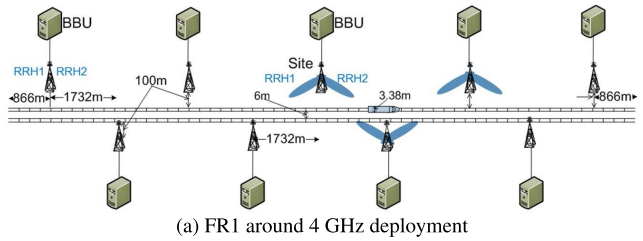

(a) FR1 around 4 GHz deployment

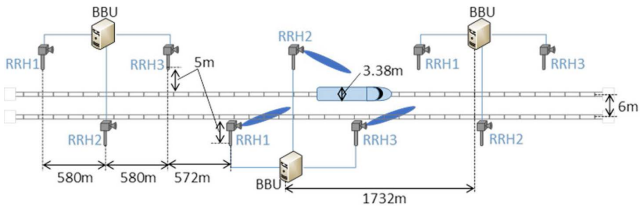

(b) FR2 around 30 GHz deployment

FIGURE 1. High-speed train deployment layout.

HST scenario aims to provide a consistent passenger user experience with very high mobility for passenger UEs located in train carriages. In the HST scenarios, two communication schemes are considered: The first scheme is direct communication between the RRH and passenger UEs in the train in FR1. The second scheme is a two-hop communication between the RRH, relay node, and passenger UE. The first hop is the communication between the RRH and relay node located at the top of one carriage of the train. The carrier frequency for the first hop is either FR1 or FR2. The second hop is the communication between the relay node and passenger UE inside the train carriage. The antennas of the relay node for the second hop can be inside the train and distributed to all carriages, as illustrated in Fig. 3 in [2] and Figs. 1, 2 in [46]. The carrier frequency for the second hop can be either FR1, FR2, or approximately 70 GHz [1]. Another issue with the linear-cell RRH deployment is whether an SFN model or non-SFN model is considered; more details can be found in [47].

The aforementioned HST deployment in 3GPP is highlighted by mobile wireless backhaul via a mobile relay on the train. Mobile relays are particularly suitable for HST scenarios. With mmWave band communication recognized as a promising technique to solve the spectrum scarcity problem as well as the more stringent throughput and delay requirements for emerging train applications, the mobile relay is a perfect tool for replacing the detrimental propagation conditions with more advantageous ones. Direct communication between the BS and UEs inside train carriages is subject to a high penetration loss in mmWave communication. Mobile relay antennas for backhauling to RRH can be installed on top of the train carriage, whereas its antennas for the access haul can be installed inside the train carriage or even in a distributed antenna system (DAS) manner in multiple trains [2], [46]. Thus, high penetration loss can be avoided. Apart from the improvement in the propagation condition, the mobile relay can also facilitate physical layer signal processing. By replacing direct communication with dual-hop communication, the high mobility issue dwells only in the first mobile wireless backhaul. Because mobile relays have a stronger power supply and more sophisticated antenna implementation, they can perform more adaptive signal processing and channel estimation. Finally, with the mobile relay, per-UE mobility management in direct communication can be replaced by a more efficient group handover [48], with the mobile relay acting as both a handover delegate point and an access point for passenger UEs in trains.

Mobile relays for HST have already attracted attention in 3GPP for LTE [49]. The work in [50] analyzed the performance of LTE mobile relays for an urban rail transportation system under loaded conditions. Thanks to the mobile relay, they have confirmed a reduction in packet loss ratio for voice communications at the expense of a slight end-to-end latency as well as a significant reduction in the load time and increase in throughput for web browsing. Channel characterization and modeling for a sub-6 GHz mobile wireless

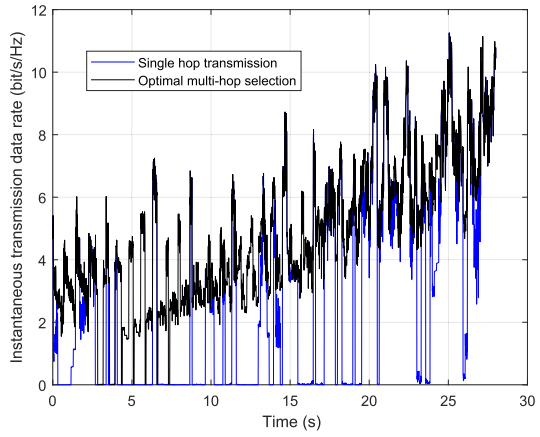

(a) Instantaneous transmission rate vs. time

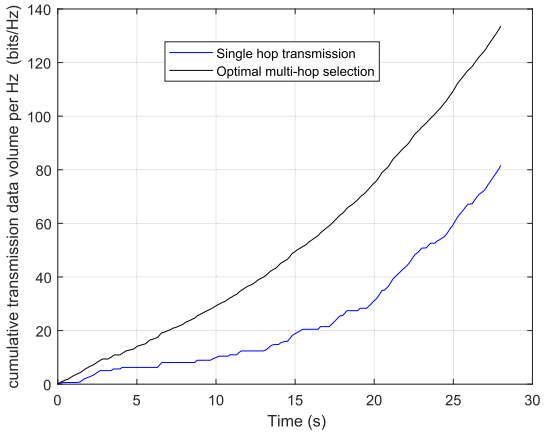

(b) Cumulative transmission data volume per Hz vs. time

FIGURE 2. Comparison between optimal multi-hop mobile relay selection and single hop transmission in HST.

backhaul have been investigated in many studies [46], [51], [52]. Measurement campaigns have been conducted for various sub-scenarios such as open space [53], viaduct [54]–[58], cutting [58]–[61], tunnels [62], and train stations [63].

Mobile relays for HST have also been extensively studied for 5G and beyond. In [6], mobile hotspot network architectures resembling the 3GPP HST scenario were proposed. In this architecture, approximately 30 GHz mmWave band communication is envisaged for mobile wireless backhaul between the RRH and relay node. A Wi-Fi-based communication is adopted for the access link between the relay node and the passenger UE. In [64], a 41 GHz mmWave band mobile wireless backhaul and Wi-Fi or small cell communication for the access link were investigated. In [65] seamless radio-over-fiber (RoF) and mmWave systems for wired optical backhauling from BS to RRH, and an approximately 90 GHz mmWave band mobile wireless backhauling from RRH to mobile relay on the train were proposed. Despite the constant attention on the mmWave band for HST in the literature, very few measurement campaigns have contributed to field measurements and channel modeling. The work in [6] measured and parametrized a 28 GHz HST channel in a rural scenario based on the QuaDRiGa [66] channel model. The low-speed measurement results were transferred to high-mobility scenario using motion-speed scaling in the geometry-based stochastic channel model. The authors in [64] conducted measurements in an urban scenario with a relative speed of 170 km/h between two vehicles. Other works, such as [67]–[73], apply the ray-tracing-based simulation approach for HST channel modeling and characterization.

Apart from the mobile relay mounted on top of the train carriage, pioneering work has analyzed the possibility of using unmanned aerial vehicles (UAVs) as mobile relays for HST in emergency or natural disaster scenarios [74].

Another advantage of mobile relays in HST is that multi-node cooperation can be used to mitigate interference and enhance transmission. The scenario proposed in 3GPP assumes only a single mobile relay located on top of train carriages. However, the benefits of implementing a single mobile relay with distributed antennas, or multiple relay nodes such as mobile relays both at the front and rear of a train, or even multiple mobile relays located on top of multiple trains have been investigated in [2], [6], [46], [75]–[80]. Two basic schemes are considered: (i) multi-hop relaying and (ii) cooperative transmission. In multi-hop relaying schemes, different metrics, such as optimal routing path selection [77], end-to-end delay [77], [78], secrecy [79], throughput [75], [77], [79], and fairness [80], as well as combinations of such metrics have been considered. Adopting the same simulation assumptions as in [75], a system-level simulation to evaluate the mobile relay multi-hop transmission is illustrated in Fig. 2. In Fig.2(a), a comparison between the optimal multi-hop mobile relay selection and single-hop transmission (with the best SNR transmit point selected) is shown. Fig. 2(b) further shows that the optimal multi-hop mobile relay selection scheme outperforms single-hop transmission in terms of cumulative transmission data volume. This is because spatial diversity can be better harvested with dynamic multi-hop mobile relay selection to overcome deep fading. In cooperative transmission schemes, DAS [2], [46] implementation and CoMP implementation [6], [46], [76] have been studied. In the DAS scheme, the antennas for a mobile relay node are physically separated to profit from uncorrelated fading at different locations. In the CoMP scheme, multiple relay nodes exist, and cooperation among them to reduce interference and enhance transmission is possible.

2) FIXED RELAY (INTEGRATED ACCESS AND BACKHAUL)

Fixed relay, better known as integrated access and backhaul (IAB) in 3GPP, is another very relevant technique for the HST scenario. Since network densification is unavoidable for mmWave band communication deployment due to its innate high path loss feature, IAB is a cost-effective implementation. Conventional wired-optical-fiber backhaul can be replaced by an equally effective wireless backhaul in the mmWave band, which significantly improves the network operator's

capital expenditure (CAPEX) and operational expenditure (OPEX).

The IAB is where wireless backhaul relaying features are currently being treated in the 3GPP. Previously, studies in wireless backhaul were known as LTE relaying in 3GPP LTE release 10 [81]. However, there has been little concern because of its rigid single-hop deployment structure, fixed connection to the parent BS, and strict resource-partitioning scheme between access and backhaul [82]. Starting from release 16, 5G NR IAB has been standardized, and continuous IAB enhancement has been investigated in release 17 and the upcoming release 18. In release 16 IAB, only the basic features and operations for multi-hop and multi-path relaying are supported [83]. The relay nodes were fixed. The mesh architecture is not supported, and only the spanning tree and directed acyclic graph architectures are supported. In 3GPP, the mobile relay is viewed as an enhancement feature for IAB and some companies have proposed IAB enhancement to support the mobile relay at the beginning of the release 17 IAB enhancement discussion [84]. However, these features have not yet been adopted. In release 17, which will be finalized shortly, IAB enhancement features including wireless backhaul duplexing, topology adaptation enhancement, routing, and transport enhancements are standardized [85]. In release 18, the mobile relay comes back as a widely recognized feature. A work item led by RAN 3 on mobile IAB and vehicle-mounted relays (VMR) was approved [86]. Use cases and potential new requirements have already been analyzed for 5G support of mobile base station relays mounted on vehicles, tramways, metros, and trains [87]. In this new work item, the goal is to define procedures for migration and topology adaptation to enable IAB node mobility, group mobility of an IAB node together with its served UEs, and interference mitigation due to IAB node mobility.

There are two types of nodes in IAB: IAB donor and IAB node. The IAB donor is the master node that provides wireless backhaul to the slave IAB nodes under its control. The IAB donor can also communicate directly with the UEs. The IAB nodes can serve as an access point to the UEs, as well as a wireless backhaul to a child IAB node. More detailed information regarding IAB architecture, functionality, and protocol can be found in 3GPP documents and surveys [82], [83], [88]–[91].

For the HST scenario, the IAB is particularly interesting for the deployment of RRH along the rail track. As is illustrated in Fig. 1(b), a dense deployment with an inter-RRH distance of approximately 600 m is assumed for FR2 mmWave band communication. Therefore, an IAB implementation that replaces the wired/RoF connection between the RRH and the base band unit (BBU) can be beneficial. The IAB deployment for RRH renders a more flexible topology management and routing path selection. It also introduces new problems for mobility management because the IAB architecture is different from conventional SFN or non-SFN architectures. Inspired by the conventional theoretical analysis of decode-and-forward (DF) relaying and amplify-and-forward (AF) relay channels in [92]–[95], existing works on IAB for HST scenarios mainly focus on how dedicated railway application requirements can be supported with an IAB-based multi-hop relaying strategy. In [96], the joint optimization of radio resources and routing paths was considered for throughput-aware or delay-aware railway applications. The railway service continuity was analyzed using OPNET simulations for the IAB-based LTE-R architecture in [97].

III. PHYSICAL LAYER ENHANCEMENT FOR HST: RECONFIGURABLE INTELLIGENT SURFACE

An old Ottoman Turkish proverb once said, 'If the mountain will not come to Muhammad, then Muhammad must go to the mountain'. MIMO techniques with different levels of cooperation are perfect examples of ''how Muhammad must go to the mountain''. To tackle the problem of fading and interference, they seek to apply appropriate signal processing on the TX/RX side to either adapt to the propagation condition or mitigate or exploit interference. However, with the advent of RIS techniques, the mountain can miraculously come to Muhammad. RISs are artificial surfaces made of electromagnetic materials that can be configured using integrated electronics. Current RIS implementations include conventional reflection-arrays, liquid-crystal surfaces, and software-defined meta-surfaces [98]. The differentiating factor for RIS from other MIMO family techniques (except relay) is as follows. Rather than working on the transmission signal, RIS makes the environment controllable by shaping the propagation channel itself. For example, the scattering, absorption, reflection, and diffraction properties can be changed over time and controlled using software [99], [100].

RIS-based transmissions have drawn considerable attention in recent years. It is widely acknowledged as groundbreaking, beyond the MIMO paradigm, which will profoundly change the wireless design beyond 5G [100]–[103]. Few studies have investigated how RIS can promote physical layer enhancement in HST. They can be categorized into the following six aspects:

A. BEAMFORMING, INTERFERENCE MANAGEMENT, AND CHANNEL ESTIMATION

The RIS can change the characteristics of propagating waves and evanescent waves with a significant loss reduction. With a passive, lossless RIS, the incident beam is first received and converted into a surface wave, subsequently guided along the surface, before it is launched back into space from a location that is electrically far from the receiving point. The power of the desired output wave was the same as that of the incident beam [104]. With multiple RIS elements, apart from the conventional array gain proportional to the number of elements N introduced by constructive superposition of multiple copies of the time-delayed signal, there is also an additional effect of signal power received from the transmitter proportional to the RIS surface area, which is also proportional to N. The combination of these two effects leads to an SNR at RX proportional to N^2, which is called the

"square law" in [105], [106] under the far-field approximation. By virtue of such an amazing feature, RIS can be used for passive beamforming such that the interference level can be reduced, and signal reception can be enhanced. In several studies, including [99], [107]–[109], the application of RIS for adaptive beamforming and interference management has been investigated for general-purpose networks. However, it has also been reported that owing to the RIS intervention on the radio propagation environment, perfect and instantaneous CSI is a prerequisite for an efficient design [107], [110]. Thus, instantaneous CSI acquisition for a real-time RIS configuration in a high-mobility scenario seems to be prohibitive because there is very rapid channel variation in a short coherent time. However, in the HST scenario, due to the regular and repetitive deployment and predictable train trajectory, an accurate and fast channel estimation is possible. The authors in [111] proposed deploying an RIS on top of the train carriage to improve the interference-resisting capacity of railway wireless communication systems. The instantaneous CSI over interference links is agnostic, and only statistical information is considered. In [112], a two-time scale channel estimation framework was proposed to separately estimate the quasi-static BS-RIS channel on a larger time scale and the fast-varying RIS-UE/BS-UE channel on a shorter time scale. It is also mentioned in [113] that prior information such as location, direction, velocity and geometry information such as angles of departure (AoD) and angles of arrival (AoA) can be obtained from an external location information system, such as a global navigation satellite system (GNSS). Such information can be used to decrease the channel estimation complexity and reduce the training overhead. In addition, compressive sensing (CS)-based channel estimations exploiting the channel sparsity for the cascading BS-RIS-UE channel in the angular domain were investigated in [112], [114]–[116].

B. THROUGHPUT AND ENERGY EFFICIENCY ENHANCEMENT

Owing to its ability to create a smart radio environment with controllable propagation conditions (referred to as the layer 0 design in [100]), the most evident feature of RIS is that it boosts the communication data rate and improves energy efficiency. Various studies have investigated RIS-aided MIMO designs for better beamforming or power allocation to optimize the system capacity or energy efficiency for general-purpose network [107], [117], [118]. The remarkable capability of RIS has also attracted the attention of researchers working on HST. In the European Commission, the Horizon 2020 project Reconfigurable Intelligent Sustainable Environments for 6G Wireless Networks (RISE-6G), an RIS-empowered use case for HST, is considered, and a field trial is planned. They will use RIS to enhance connectivity in a train station for three purposes [119]: i) coverage optimization for indoor shops, ii) dedicated resting areas for instant video download and cloud gaming ensuring the highest bandwidth and network efficiency, and iii) EMF limitations in private areas or for workers protection purposes. In [120], [121], the authors pointed out that the HST communication network has distinct requirements compared with the general-purpose public wireless network. The required throughput and connection density are non-uniformly distributed, with a specific repetition pattern, and are only concentrated in the area close to the rail tracks. Thus, with a priori knowledge of the train velocity and trajectory, the RIS can control the direction and shape of the impinged waves such that the communication channel spectrum or energy efficiency can be optimized.

C. DOPPLER COMPENSATION

The Doppler shift in the HST scenario is severe, considering the speed of trains up to 500km/h. In addition, the multi-path signals will have distinct velocity vector projections on the angle of arrival for each cluster and ray, adding the problem of Doppler spread on top of the time-varying Doppler shift and making the Doppler compensation even more difficult. Before RIS was born, it was reported in [122], [123] that Doppler shift tracking and compensation in LTE-R-based HST systems can be facilitated with the repetitive and predictable Doppler introduced by deterministic train trajectory, standard dimension tracks, and repetitive movements of trains along fixed tracks. With RIS techniques, considering only RX mobility, the Doppler shift for RIS element n and an arbitrary propagation path can be denoted as

$$\begin{aligned} f_d &= -\frac{d}{dt}\left[f_c\left(\tau_{n,a} + \tau_{\theta_n}(t) + \tau_{n,b}(t)\right)\right] \\ &= -f_c\frac{d\left(\tau_{\theta_n}(t) + \tau_{n,b}(t)\right)}{dt}, \end{aligned}$$

where f_c is the central frequency, $\tau_{n,a}$ is the delay of arbitrary path among the L_a path between TX and the n-th element of RIS, $\tau_{n,b}$ is the delay of an arbitrary path among the L_b path between the n-th element of RIS and RX, τ_{θ_n} is the delay introduced by the n-th element of RIS with configuration $\theta_n \in \Omega$ lying in the entire feasible configuration space Ω. The Doppler shift can be easily compensated by tuning the RIS-induced delay such that

$$\frac{d\left(\tau_{\theta_n}(t)\right)}{dt} = -\frac{d\left(\tau_{n,b}(t)\right)}{dt}.$$

This is known as Doppler cloaking [100]. The Doppler spread introduced by the multi-path effect can be handled by RIS techniques in the HST. This is because in the HST scenario, the main scattering objects are generally of a regular shape and are easy to identify. Therefore, it is possible to deploy RISs along the tracks or on top of train carriages [111], [121] to compensate for and align the Doppler shift from different multi-path components. In [124], the authors studied RIS optimization with predictive mobility compensation to maximize the receive power and minimize the Doppler spread and shift for low Earth orbit satellites. The proposed method can also be applied to other communication scenarios with both mobility and predictable trajectories such as HST.

In addition to the conventional Doppler effect due to high mobility, another typical Doppler-related problem in the HST scenario is the abrupt jump in the Doppler shift [121]. There was a sudden change in the sign of the Doppler shift from $+f_d$ to $-f_d$ the moment when the train passed the RRH. Because of its high mobility, it is difficult to detect and compensate for such phenomena in a time-effective manner. In [121], the use of multiple RISs to suppress such a Doppler jump was proposed. When a train passes an RIS, passenger UEs inside the train carriages that have already passed the RIS will be served by another RIS. The Doppler shift will also be estimated using this other RIS. The RIS at the passing point will only be used to estimate the Doppler shift for the passenger UEs inside the train carriages that have not yet passed the RIS.

D. NETWORK DEPLOYMENT OPTIMIZATION

Similar to relay techniques in MIMO, RIS exhibits good features in terms of network deployment optimization, such as coverage extension, blockage, and dead zone suppression. An RIS can be viewed as a transparent relay with a full-duplex protocol that affects the propagation condition in real time [102], [106]. Several studies [102], [106], [109] have compared RIS techniques with conventional transparent relay (e.g., AF relay) and regenerative relay (e.g., DF relay) techniques. The work in [106] has demonstrated that DF relay consistently provides a better end-to-end SNR than RIS, even though RIS benefits from a "square law" in terms of RIS element numbers in the far-field approximation. However, the RIS remains advantageous due to its low complexity and low energy consumption. For a general-purpose network, RIS can be properly deployed to enhance coverage [125] and combat the blockage of mmWave communications by creating an additional virtual line-of-sight (LoS) path [126]–[128]. In the HST scenario, based on statistical CSI, [129] proposed an IRS-assisted communication system model to relieve blockage issues in terms of the outage probability. In [113], [121], applying RIS for coverage extension, frequent handover reduction, blockage, and dead zone suppression in HST scenarios was thoroughly investigated. Two types of RIS deployments have been discussed: i) RIS deployed on one side of the rail track, for example, on a roadside advertising board as a reflective panel [113], [129]. ii) RIS deployed on top of train carriages. In these deployments, replacing the mobile relays with RIS or a combination of mobile relays and RIS are two possible strategies. Additionally, both passive and active RIS can be used [121]. To summarize, RIS-aided HST network deployment optimization has two major advantages: (1) RIS integration has little impact on the current HST network infrastructure because of its feature called layer 0 smart radio environment design [100]. (2) The RIS is beneficial in terms of CAPEX and OPEX management because it is a low-cost, passive, or low-power consumption device that can plug and play.

E. PENETRATION LOSS REDUCTION

Not only can the RIS reflect the impinging waves towards dedicated directions, but it is also capable of refracting the signal towards specified directions that do not necessarily adhere to the laws of refraction [109], [130]. This feature can be beneficial in the HST scenario which suffers from severe penetration loss of outdoor-to-in-train communication for UEs located in train carriages. Most commercial train carriages are made of aluminum alloy or stainless steel. Table 1 captures the measurement result of the average penetration losses for different off-the-shelf train carriages. This reveals that the metal train carriages are rather difficult to penetrate for sub-6 GHz signals, let alone mmWave band communication. However, it was reported in [121] that penetration loss varies as a function of the angle of incidence. A larger incidence angle led to a higher penetration loss. The smallest penetration loss is obtained when the incident wave is perpendicular to the surface. Therefore, the authors in [121] suggested that the penetration loss for a BS for in-train UE communication can be reduced by dynamically controlling the angle of incidence for trains appearing at the cell edge.

TABLE 1. Penetration loss of HST commercial train carriages in 2.6 GHz, table adapted from [131].

Train type	Material	Average penetration loss (dB)
CRH1 (Bombardier)	Stainless steel	26
CRH2 (Kawasaki)	Aluminum alloy	18
CRH3 (Siemens)	Aluminum alloy	22
CRH5 (Alstom)	Aluminum alloy	26
CRH380A (CSR)	Aluminum alloy	30
CRH380B (Siemens)	Aluminum alloy	28
CRH380C (Hitachi)	Aluminum alloy	26
CRH380D (Bombardier)	Aluminum alloy	26
CRH6 (CSR)	Aluminum alloy	18

Apart from the metal-based structure of the train body, glass windows are deployed in train carriages. Compared to metallic materials, glass has a much lower penetration loss. In 28 GHz and 38 GHz, a 1 cm thick glass window has a penetration loss of 1.38dB and 3.72dB, respectively [132]. In addition, a larger angle of incidence leads to a higher penetration loss. In [121], the authors also mentioned that the refraction coefficient was affected by the angle of incidence for impinged waves with different polarization directions. The refraction coefficient of a vertically polarized signal decreased linearly as the angle of incidence increased. However, for a horizontally polarized signal, the refraction coefficient is insensitive to the angle of incidence. As a result, when combined with RIS, distinct polarization states can be applied for signal refraction enhancement under different propagation circumstances and this technology seems to be promising when combined with polarization diversity transmission. An RIS deployment attached to the external surface of a train window to promote signal refraction was proposed in [113], [121]. If the RIS is active and dynamically

configurable, additional beamforming can be applied to serve the UEs located at different positions inside the train.

F. RIS-AIDED LOCALIZATION AND SENSING

Localization (sensing) is used to estimate and track the position of an active (passive) object. In any localization and sensing system, there are three essential parts: measurements, reference system, and inference algorithm [133]. The positioning reference signal (PRS) in the downlink and sounding reference signal (SRS) in the uplink are the physical layer reference signals used for positioning in 5G networks. Time measurements such as time-of-arrival (TOA) and round trip time (RTT), angular measurements such as AoA and AoD, and power measurements such as reference signal received power (RSRP) can be used for positioning. The reference system can be the BS, where geographical information is assumed to be known. Different measurements are required for different inference algorithms. Apart from physical layer reference signals for positioning, GNSS-based positioning, such as GPS, has also been considered for 5G. RIS-aided localization and sensing are beneficial for all the three essential parts. The location of the RIS can serve as a secondary reference system to improve the localization and sensing accuracy. With RIS providing supplementary measurements for additional propagation paths, more sophisticated and precise inference algorithms can be used for better localization and sensing. Some surveys and tutorials on RIS-aided localization and sensing can be found in [100], [133].

In HST scenarios, RIS-aided localization and sensing are relevant for physical layer enhancement. As is mentioned in Sections III-A and III-B, positioning information can help beamforming and channel estimation, thereby rendering better throughput and power efficiency in HST communication. However, localization and sensing in HST can be quite challenging owing to their high mobility. A more stringent delay and reference signal robustness in terms of high mobility are required. Therefore, the inclusion of RIS in HST localization and sensing is very promising due to the unparalleled enhancement of all three essential factors. To the best of our knowledge, only the work of [121] has pointed out the potential benefit of applying RIS for localization and sensing in HST. However, detailed algorithms and evaluations remain uncharted and should be investigated in the future.

IV. PHYSICAL LAYER ENHANCEMENT FOR HST: REFERENCE SIGNALS AND WAVEFORM DESIGN

As mentioned in I-A, the high-mobility induced Doppler effect and high-frequency induced phase noise are two challenges in the HST physical layer design. In 3GPP NR specifications, high mobility issues are mainly treated in V2X applications to consider the Doppler effect stemming from a substantial increase in vehicle velocity. Previous releases of 3GPP had already provided a reference signal design to deal with the time variations of the channel. However, in contrast to the NR, the design was almost static. The flexibility of NR partly remains in numerous forms of leverage to make transmission more robust against many phenomena. Among them, phase noise, whose emergence is closely linked to the increase in carrier frequency, is one of the main goals of NR 5G and beyond.

In the following paragraphs, we first describe the reference signal design in NR for channel estimation, which requires a brief introduction of the method of control channel allocation. It should be noted that this reference signal design originally targeted high-mobility V2X sidelink communication in 3GPP. They are also relevant for HST T2I and T2T communications if a sidelink is used. For an eMBB-based design, the interested reader can refer to [134]. Second, phase noise compensation is presented through the associated NR reference signals.

A. PHYSICAL SIDELINK CONTROL CHANNEL (PSCCH)

PSCCH significantly differs from the physical downlink control channel (PDCCH) used in eMBB scenarios [135], [136]. In sidelink scenarios, a frequency resource is defined in several subchannels, where a subchannel is a contiguous collection of physical resource blocks (PRBs). Regardless of the type of channel to allocate, the PSCCH, or the physical sidelink shared channel (PSSCH), the physical channel is mapped on a finite number of subchannels. The specifications require a single subchannel, as mentioned in [137], to reduce the blind decoding complexity of the UEs. For a large subchannel length, the PSCCH spreads within numerous PRBs. To contain the payload of the PSCCH, the associated number of OFDM symbols is small (e.g., two OFDM symbols). In contrast, for a small subchannel length, the payload of the PSCCH requires more OFDM symbols to be entirely contained, e.g. three OFDM symbols. Fig.3 shows an example of a PDCCH allocation and Fig.4 shows an example of a PSCCH allocation.

FIGURE 3. PDCCH for eMBB.

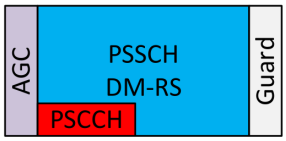

FIGURE 4. PSCCH for sidelink. The automatic control gain symbol (AGC) helps calibrate the power at the receiver side. The guard symbol is a Tx-Rx switching time margin.

B. DEMODULATION REFERENCE SIGNALS (DM-RS) PATTERNS DESIGN

In eMBB, the PDCCH spreads within the full frequency allocation regardless of the number of OFDM symbols and

payload. Therefore, the first OFDM symbols of any slot are dedicated to PDCCH and the remaining OFDM symbols are dedicated to data and reference signals, that is, the so-called DM-RS. The DM-RS then occupies the full OFDM symbols.

An important feature of NR, compared with LTE, is the possibility of allocating slots of various sizes, from 2 to 14 in eMBB and from 6 to 13 in sidelink. Several DM-RS patterns are accordingly defined to fit with every slot size, comprising a degree of freedom to deal with various channel conditions, for example, the Doppler effect due to high speed. In eMBB, regardless of the pattern, a DM-RS symbol is systematically allocated to the first OFDM symbol immediately after the PDCCH. This front-loaded DM-RS allows any terminal to trigger an early channel estimation that permits the progressive and faster demodulation of the data symbols. In low-speed scenarios, the channel is not expected to vary significantly from slot beginning to slot end. Therefore, for a sufficiently high SNR, there is no need to allocate more than one DM-RS symbol, and the front-loaded DM-RS is sufficient to efficiently track the channel. However, in a high-speed scenario, the Doppler effect exerts a noticeable influence on the temporal nature of the channel such that a channel interpolation process is required within a slot. This is enabled by allocating at least two DM-RS symbols within the slot. The specification allows for up to four DM-RS symbols in the case of long slots, which are nearly evenly distributed within the slot.

Considering the sidelink scenarios where the speed reached by vehicles is often much greater than in the eMBB scenarios, considering that the PSCCH only spreads over a single subchannel, and considering the possibility that the PSCCH may spread over more than two OFDM symbols, it is necessary to allocate DM-RS in OFDM symbols to be used for PSCCH and in OFDM symbols to be used for PSSCH. Consequently, the DM-RS symbols allocated with PSCCH symbols are truncated or partially overwritten by the PSCCH. If only two DM-RS symbols are allocated, the specification establishes the possibility of shifting the front-loaded DM-RS symbol provided that the slot length is nine at least. The rationale behind this is that the second DM-RS symbol, which is allocated quite close to the last OFDM symbol of the slot, is far enough from the first DM-RS symbol to avoid a significant loss in the performance.

The specification allows from two to four DM-RS symbols in a sidelink slot. If the number of DM-RS is three, which is possible for a slot length greater than or equal to nine, or if the number of DM-RS is four, which is possible for a slot length greater than or equal to eleven, there is a front-loaded DM-RS. This ensures a sufficient distance between the DM-RS symbols to benefit from interpolation. However, this also implies that DM-RS is truncated. At least two alternatives can be envisioned to avoid front-loaded DM-RS truncation. The first is to shift the front-loaded DM-RS to the OFDM symbol immediately after the last PSCCH symbol. However, the distance to the next DM-RS symbol is so small that the interpolation becomes pointless. Moreover, the near-DM-RS symbols are not more efficient than a single one, and the associated overhead is only a burden that reduces the throughput. The second alternative consists of removing the front-loaded DM-RS while ensuring a DM-RS immediately after the last PSCCH symbol. This creates an imbalance between the PSSCH symbols dwelling between the DM-RS symbols and benefit from the channel interpolation, and PSSCH symbols which dwell before the first DM-RS symbol. In the case of a high Doppler effect, these symbols suffer from high degradation which leads to poor performance. Finally, truncation of the front-loaded DM-RS symbol proved to be the best trade-off. Fig.5, Fig.6, and Fig.7 show examples of DM-RS allocations considering, for each of them, in a particular case.

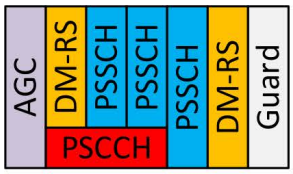

FIGURE 5. Short slot. 2 DM-RS only. The interpolation is possible only with a truncated front-loaded DM-RS symbol.

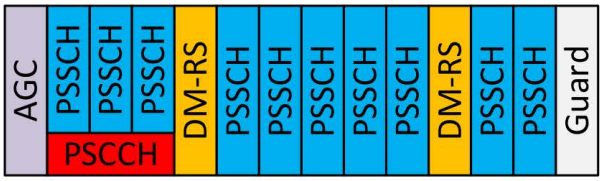

FIGURE 6. Long slot. For low speed, 2 DM-RS are enough to cover the whole slot. The front-loaded DM-RS symbol is shifted because no performance loss is expected in the interpolation and the edge extrapolation.

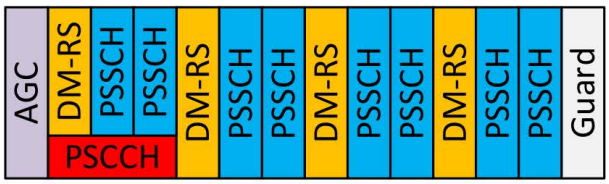

FIGURE 7. Long slot. For high speed, 4 DM-RS are necessary to track time variations of the channel over the whole slot. The front-loaded DM-RS symbol is truncated since it cannot be shifted to keep an interpolation gain.

C. DEMODULATION REFERENCE SIGNALS (DM-RS) PATTERNS SELECTION

In the sidelink, the UE is responsible for the DM-RS pattern that it allocates in the slot. There are no rules in the specifications to guide the UE, except for the table of allowed DM-RS patterns [135]. The UE selects a DM-RS pattern within a

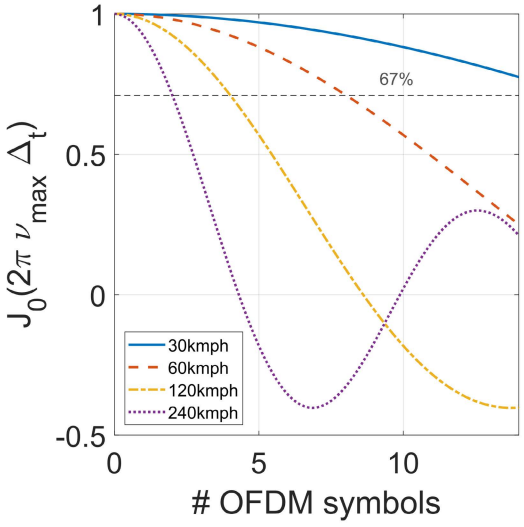

FIGURE 8. Autocorrelation of the channel against the time separation in the number of OFDM symbols. One DM-RS every 2, 4, and 8 symbols would be required for a relative speed of 240 km/h, 120 km/h, and 60 km/h, respectively. Only a single DM-RS would be necessary for 30 km/h.

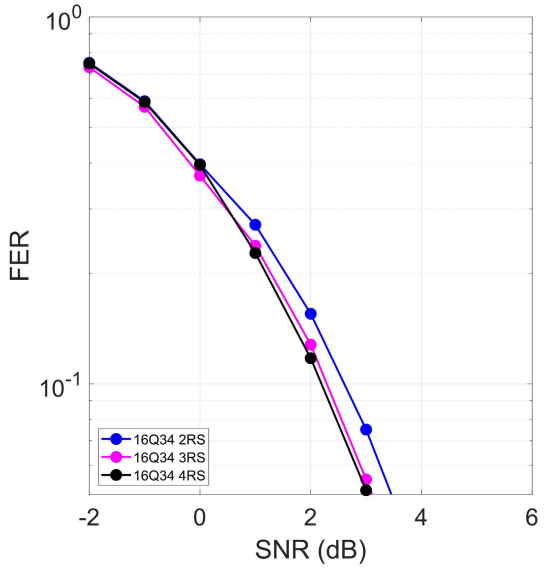

FIGURE 9. Performance for a subcarrier spacing of 15 kHz with a relative speed of 40 km/h between two vehicles.

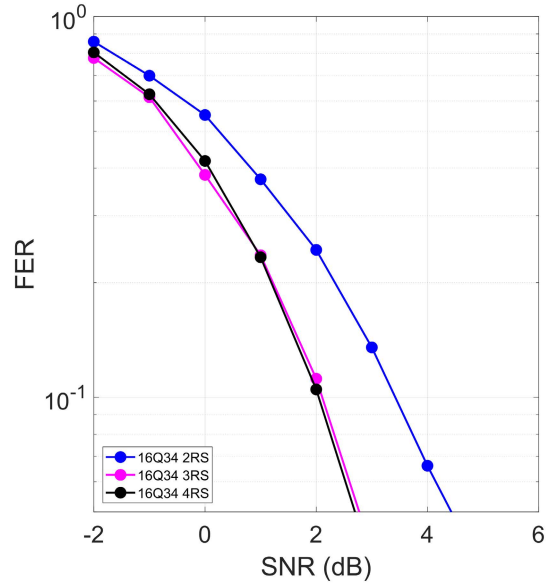

FIGURE 10. Performance for a subcarrier spacing of 15 kHz with a relative speed of 120 km/h between two vehicles.

set defined for each resource pool. The UE determines the DM-RS pattern within the specified patterns, based on individual considerations. Among the various possibilities, the UE considers the modulation and coding rate (MCS) and speed as crucial parameters for selecting the best DM-RS pattern.

First, given the slot length, number of subchannels, and number of PSCCH symbols, the number of DM-RS symbols is the last variable that determines the exact available space for the data. Provided the data payload, it is possible to select the MCS to be applied to fit this space. With a different number of DM-RS symbols, for the same data payload, another choice of MCS arises.

Second, the channel time variations are closely related to the velocity v such that they significantly vary from one OFDM symbol to the next when increasing the speed. The Doppler effect is mostly modeled by the Jakes'model [138], the autocorrelation function of which is the first-order Bessel function $J_0(2\pi\,\nu_{max}\,\Delta_t)$ where $\nu_{max} = vF_c/c$ is the maximum Doppler shift, F_c is the carrier frequency and Δ_t is the time separation. Owing to this model, the interval Δ_t^* between two consecutive DM-RS can be selected to ensure an arbitrary coherence time. One can see for example Fig.8 which illustrates the best separation for $J_0(2\pi\,\nu_{max}\,\Delta_t^*) \geq 67\%$. This explains the need to get DM-RS at positions 3, 6, 9, and 12 in an LTE V2X subframe where the expected speed may reach up to 140km/h. Consequently, DM-RS-based channel estimation is more efficient with more DM-RS symbols because the coherence time between any two consecutive DM-RS remains sufficiently high. Finally, the UE must consider the speed and the remaining payload in accordance with the number of DM-RS symbols.

To reflect the dependence on the Doppler effect, Fig.9, Fig.10, and Fig.11 exhibit the FER performance for various DM-RS patterns given low, moderate, and high speeds [139]. The evaluation assumptions are compliant with the 3GPP assumptions, including the baseline Rel-15 NR PUSCH design, considering some details available in [140].

The slot duration was shorter for a higher subcarrier spacing. Consequently, the Doppler effect has less impact on the performance, which allows a reduction in the number of DM-RS symbols to be allocated within the slot. The selection

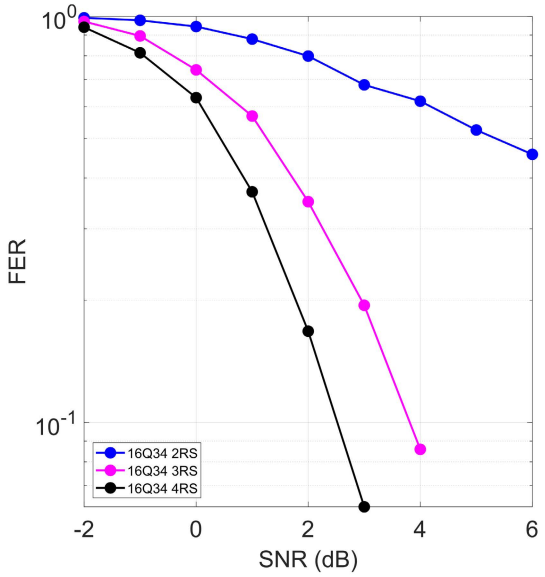

FIGURE 11. Performance for a subcarrier spacing of 15 kHz with a relative speed of 240 km/h between two vehicles.

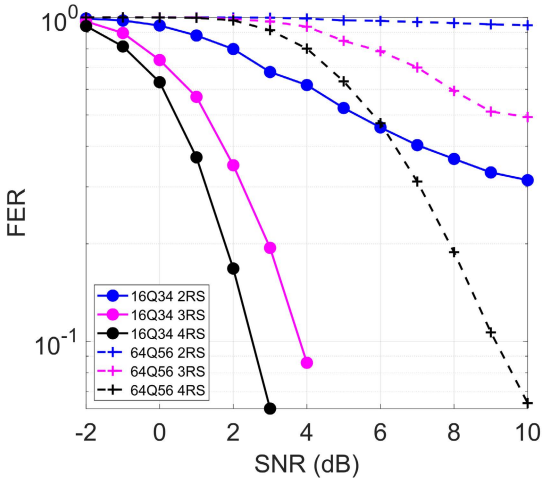

FIGURE 12. Performance for a subcarrier spacing of 15 kHz with a relative speed of 240 km/h between two vehicles.

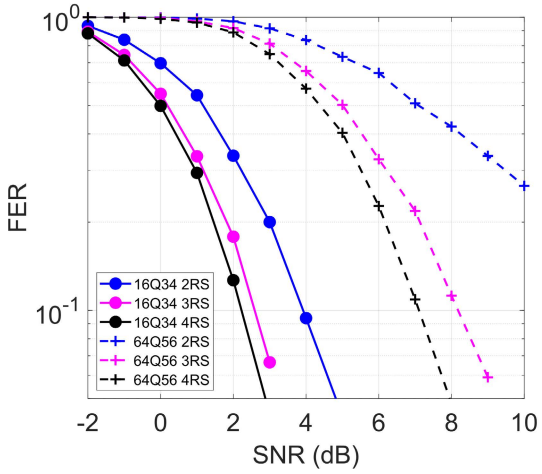

FIGURE 13. Performance for a subcarrier spacing of 30 kHz with a relative speed of 240 km/h between two vehicles.

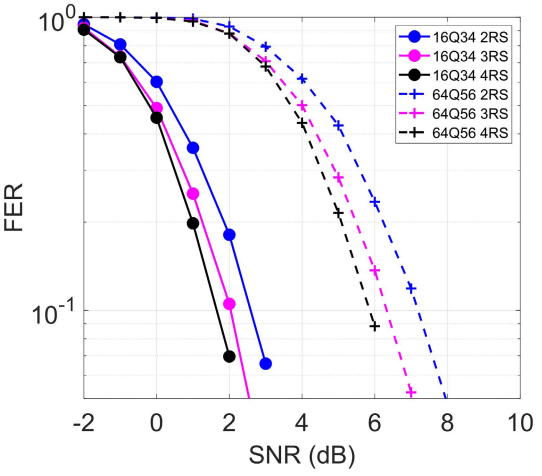

FIGURE 14. Performance for a subcarrier spacing of 60 kHz with a relative speed of 240 km/h between two vehicles.

of the DM-RS pattern should then consider the numerology of the resource pool and the relative velocity of the vehicles. This is shown in Fig.12, Fig.13, and Fig.14 where the subcarrier spacing lies within 15 kHz, 30 kHz, and 60 kHz, respectively, and the relative speed is 240 km/h. Three MCS were evaluated, each with three DM-RS patterns.

D. PHASE TRACKING REFERENCE SIGNALS (PT-RS)

In NR Rel.15/16, PT-RS was introduced to combat the phase noise, which turned out to be very strong when the carrier frequency was increased to mmWaves. Phase noise is a synchronization impairment stemming from local oscillators [18], [141]. The DC components of the phase noise generate a common phase error (CPE) that is identical to all subcarriers and time instants in an OFDM symbol. The time-variable phase noise components within a single OFDM symbol lead to inter-carrier interference (ICI). The received symbol Y_k at subcarrier k after channel estimation but before phase noise compensation can be modeled as follows:

$$Y_k = \Psi_0 X_k + \sum_{j>1} \Psi_j X_{<k-j>_N} + Z_k, \tag{1}$$

where X_k is the emitted signal at subcarrier k, Ψ_j is the phase noise at subcarrier j, and Z_k is the additive white Gaussian noise (AWGN) at subcarrier k, and all the three previous symbols are in frequency domain. $< . >_N$ is modulo N where N is the order of the Fourier transform.

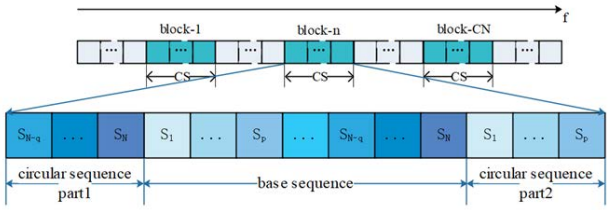

FIGURE 15. Block-based PT-RS pattern proposed in [142] to replace the Rel.16 distributed pattern.

For carrier frequencies below 52.6 GHz, the phase noise is mostly represented by its DC component Ψ_0 that impacts all received symbols with the CPE. The secondary components $\Psi_{j,\forall j>1}$ are much lower than Ψ_0 therefore the summation term in (1) can be merged with AWGN. The Rel.16 PT-RS pattern, in which one single PT-RS symbol is allocated every two or four RBs, was designed to compensate for CPE.

When working with higher frequencies, ICI cannot be considered as part of AWGN because it strongly affects the signal even more than CPE. One method to circumvent this problem is to increase the subcarrier spacing. A greater subcarrier spacing reduces the phase noise effect as the power spectral density of the phase noise converges to a single peak, that is, Ψ_0, as if the carrier frequency is lower. However, for UEs supporting a band in the range of 52.6 GHz-71 GHz that are not required to support subcarrier spacing superior to 120 kHz, the system performance needs to be guaranteed with the mandatory 120 kHz subcarrier spacing where Ψ_0 is not the sole representative of the phase noise. Therefore, sticking with the Rel.16 design without increasing the subcarrier spacing could lead to performance degradation, provided that the receiver processing targets only simple CPE compensation.

The distributed PT-RS of Rel.16 can be used to better defeat the phase noise. Because the phase noise is applied as a convolution in the frequency domain, using the PT-RS to perform a deconvolution process is suitable.

Some works [142], [143] have also proposed changing the distributed PT-RS pattern to a block-based pattern. The rationale behind this is to combat the major components around Ψ_0 relying on the contiguous PT-RS symbols. Indeed, with the power spectral density of the phase noise being a decreasing exponential function, the major power lies only around Ψ_0. One example of such a candidate is shown in Fig.15. The cyclic nature of the pattern imitates the cyclic prefix advantage in the sense that interference from neighboring symbols is absorbed.

Despite the performance enhancement compared to the Rel.16 pattern with a Wiener filter shown in Fig.16, the specification impacts might be too substantial [144].

Owing to the fast time-varying nature of the phase noise, adjacent OFDM symbols experience different ICI. Consequently, the PTRS must be allocated to every non-DMRS OFDM symbol. For Rel.16, the specifications are defined such that PT-RS does not collide with other reference

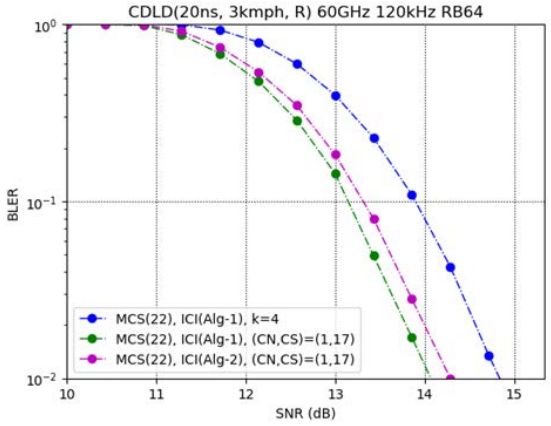

FIGURE 16. Performance of block-based PT-RS pattern proposed in [142] with two receiver processings (ICI(Alg-1) and ICI(Alg-2)) in comparison with Rel.16 with one PT-RS every 4 RBs (k = 4) at 60 GHz.

signals, for example, reference signal for tracking (commonly referred to as the tracking reference signal, TRS). However, block-based PT-RS can frequently collide with other existing NR reference signals with no simple solution; see the TRS illustrated in Fig.17. Because there are only three subcarriers between the two TRSs, there is not enough room to insert the required signal to perform well with the block-based PT-RS. Therefore, the Rel.16 PT-RS design was adopted as the Rel.17 PT-RS design.

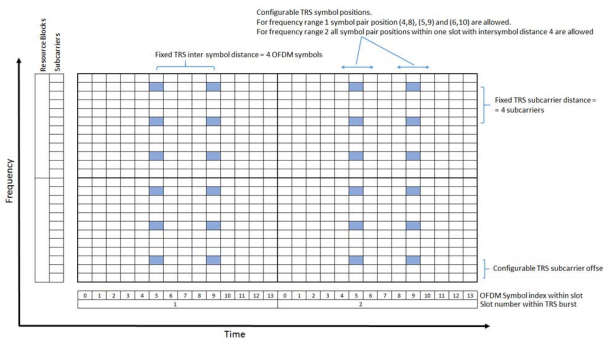

FIGURE 17. Tracking reference symbol (TRS) mapping in NR.

E. WAVEFORM FOR HST

Due to the high Doppler effect as well as the high mobility which leads to rapid channel variation and frequent channel estimation, the waveform for the HST scenario has been meticulously revisited by academies, industries, and standardization bodies. At the beginning of the HST scenario discussion in 5G, different possible waveforms for the HST were investigated. The work in [45], [145] studied the unique word embedded DFT-s-OFDM (UW-DFT-s-OFDM) waveform for HST. Various subcarrier filtering-based waveforms such as filter bank multi-carrier (FBMC), generalized frequency division multiplexing (GFDM), and subband filtering based waveforms such as universal filtered multi-carrier

(UFMC) and resource block filtered OFDM (RB-f-OFDM) have been surveyed in [146], [147]. In 3GPP, after leveraging the performance of different waveforms and the complexity of introducing a new waveform in the specification, it is decided that only DFT-s-OFDM and cyclic prefix OFDM (CP-OFDM) are used. Hence, there was no specific waveform design for the HST scenario.

F. NUMEROLOGY FOR HST

Numerology optimization for HST use cases has also been extensively investigated for 3GPP. As mentioned in [148], a large value of sub-carrier spacing (SCS) may be suitable for HST slices that require low latency, because a large SCS reduces the OFDM symbol and slot durations. A thorough study has been performed to evaluate numerology-related parameters including SCS, fast Fourier transform (FFT) size, symbol length, and CP length in HST because there are several causes of performance impairments such as Doppler shifts and phase noise in such scenarios [148], [149]. In [148] it was shown that the choice of SCS for the HST scenario should consider the Doppler shift or Doppler spread. To avoid Doppler-induced ICI, a larger SCS was used to maintain a shorter OFDM symbol duration. In addition to the Doppler effect, the effect of phase noise is significant in mmWave bands owing to the hardware limitations. Implementing an RF oscillator with low-phase-noise characteristics in the mmWave band is difficult. In October 2016 at the RAN1#87 meeting, it was agreed that extended CP for an SCS of 60 kHz is supported because it is favorable for the HST scenario.

V. PHYSICAL LAYER ENHANCEMENT FOR HST: ARTIFICIAL INTELLIGENCE AND MACHINE LEARNING ASSISTANCE

Recent years have seen a barrage of research domains waving the flag of artificial intelligence (AI) and machine learning (ML), exploiting these technologies to tackle some long-existing problems from a new angle. AI and ML have attracted the attention of researchers in the wireless communication domain, leading to a flurry of work on AI/ML assistance in physical layer design. Excellent surveys and tutorials on different aspects of physical layer design with AI/ML exist [150]–[155] and interested readers are encouraged to take a further look into them. From our point of view, three fundamental facts make AI and ML handy for physical layer problems in wireless communication.

- There is a deep connection between ML/AI and the fundamental problem of communication [151]. The detection and quantization procedures in a communication system are typical classification problems in ML. The coding and decoding procedures serve the same purpose as an autoencoder to provide accurate and robust dimension reduction and reconstruction. Pilot-based channel estimation is a supervised learning procedure for determining a linear system based on training and pilot data. The so-called team decision and decentralized control [151] for various multi-agent decision-making problems such as precoding, resource allocation, and congestion control are conventional reinforcement/ distributed/ federated learning problems. These profound and innate connections make AI/ML perfectly suitable for solving physical layer communication problems.
- Conventional blockwise split signal processing is suboptimal [150]. Current communication system designs tend to split signal processing into a chain of multiple independent blocks with different functionalities. This approach is efficient and controllable, but cannot provide optimal end-to-end performance. For example, the separation of source and channel coding for many practical channels, short block lengths, and separate coding and modulation are suboptimal [150], [156], [157]. A non-modular system with better end-to-end performance can be achieved with the AI/ML-based algorithm to learn the entire communication system.
- Under certain conditions, a data-driven approach may be better than a model-based approach. With the rapid growth of new applications with distinct requirements for various communication scenarios, we must multiply the models to precisely target each dedicated case in the conventional communication design. However, an increasing amount of data of all kinds are available on various smart devices and Internet-of-Things (IoT) objects. When the model-based approach becomes too complicated, intractable, or unable to the capabilities and requirements of devices in a fast-varying environment, a data-driven approach with AI and ML might be a better choice.

A. AI/ML FOR HST PHYSICAL LAYER: ADVANTAGES AND CHALLENGES

In HST scenarios, it is also very popular to apply AI and ML techniques to dedicated railway applications. AI/ML assistance in automatic train control (ATC), ATO, ATP, and traffic management such as train scheduling and timetable planning has been extensively investigated [158]. For researchers working on HST physical layer design, the advent of AI and ML also has also shed some light on old problems. Before investigating dedicated physical layer problems with their AI/ML-aided solutions, we would like to point out several facts that have rendered AI/ML assistance in HST physical layer design particularly effective or challenging.

First, HST physical layer design generally involves multi-dimensional, non-convex, nonlinear problems that have complex and intractable solutions. Owing to the complicated and fast-varying channel conditions, nonlinear behaviors of certain electronic devices, and hybrid analog-digital architecture in mmWave band communication systems, HST physical layer designs such as hybrid beamforming, power allocation, channel estimation, and Doppler estimation are likely to be intractable. One of the advantages of AI/ML techniques is

their ability to 'invert' sophisticated nonlinear systems and provide a good solution.

Second, in the HST scenario, some dedicated applications are delay stringent, which cannot allow accurate channel estimation. The short block length codes for such URLLC scenarios cannot benefit from the ergodicity of randomness in the channel. Therefore, these delay-aware applications in HST make the conventional blockwise, multi-layer communication architecture highly suboptimal. For example, in the HST scenario, due to the high mobility feature, conventional channel estimation, CSI feedback, and precoder design may not work properly. A joint CSI feedback compression and reconstruction, or even a joint channel estimation and signal detection design with AI/ML assistance, might be more beneficial.

In addition, a conventional model assumption in a general-purpose network may be invalid in HST scenarios. For example, owing to the extreme environmental conditions in the HST, the interference and noise can be highly non-stationary and non-Gaussian distributed. Moreover, multiple sub-scenarios exist, such as viaduct, cutting, and tunnel. Different sub-scenarios have distinct propagation conditions; therefore, dedicated models are required for the conventional physical layer design. However, such a model can be quite specific, as it only works properly for a given scenario and is difficult to generalize. Therefore, a less structured solution that is robust to model mismatch is beneficial in HST.

Despite the advantages of AI/ML in HST physical layer design, this does not necessarily indicate that AI/ML is a panacea for HST. The most evident challenge is the black-box nature of certain AI/ML algorithms [151]. Compared with the practical side, there is a clear lag in the theoretical tool development in ML. One esteemed researcher in the domain has even stated that ''Machine learning has become alchemy,'' which has clearly expressed his concern about the non-adequate research effort on ML interpretability. The most important aspect of the HST is its nature as a public safety service. Therefore, compared with other eMBB use cases where a service interruption is merely a customer satisfaction issue, it can be living or dead in the HST. Therefore, the delay and reliability requirements for certain dedicated HST applications are extremely stringent, and a black box that cannot demonstrate clear reliability and performance bounds is not acceptable.

Another challenge comes from the HST datasets. A few wireless signal datasets are available for performance evaluation and algorithm comparison in general-purpose networks [151]. To the best of our knowledge, no HST-related datasets have been identified in the literature. Other reasons have contributed to the unavailability of the HST datasets. The measurement campaign in the HST is expensive and difficult because of the high mobility and the various sub-scenarios involved. In the mmWave band and beyond, field measurement is even more difficult because of the limited channel sounding methodologies. Even if there is data available for HST, there also exists the problem of data heterogeneity, in which multiple sub-scenarios such as viaduct, cutting, and tunnel can be involved. Different sub-scenarios have distinct propagation conditions; therefore, data labeling and prepossessing are required.

Finally, there is the problem of training efficiency and AI/ML model reliability for HST. HST channels are often non-stationary. A specific deployment architecture, as well as weather conditions such as rain or snow, instantaneously affect the channel. Therefore, even if a sub-scenario dedicated neural network has been trained and calibrated with offline datasets, online training for neural network adaptation is still necessary. Unfortunately, the training time of a neural network with reasonable performance is often beyond the operational timescales of communication systems [151].

B. AI/ML FOR HST PHYSICAL LAYER: CASE STUDIES

AI/ML assistance in HST physical layer design is a nascent technique with only a few researchers recently exploring it. Nevertheless, this is a very promising research direction with good primary results. In this subsection, we briefly present case studies targeting four different topics of AI and ML assistance for HST physical layer design.

1) AI/ML ASSISTANCE IN HST CHANNEL MODELING

Channel modeling in the HST scenario for mmWave bands and beyond is challenging. There are dozens of specific sub-scenarios for HST communications with distinct propagation characteristics. Channel sounding measurements are scarce and difficult to obtain owing to the limitations of the channel sounding equipment for mmWave bands and beyond. To resolve these problems, an innovative HST mmWave band and beyond channel modeling paradigm was proposed in [5], [159]. Only a limited number of channel sounding measurements have been obtained. A ray-tracing-based simulation that serves as a channel propagation digital twin of the measurement campaign was built. The electromagnetic parameters in the ray-tracing simulation were calibrated using a limited number of channel sounding measurements. Once the ray-tracing simulation is calibrated, a massive amount of synthetic channel impulse response data can be generated. Such data can be used for channel modeling to determine channel parameters based on a selected channel model. In this new channel modeling paradigm, there are two parametrization procedures: calibration of electromagnetic parameters for ray-tracing simulation and parametrization of channel parameters for channel modeling. Both statistical and AI/ML-based approaches can be envisaged for parametrization procedures. In [160], grouping multi-path components with similar ToA and AoA into a cluster was formulated as a classification problem. Unsupervised learning with a clustering algorithm using the multi-path component distance density was applied. An ML-based approach was used to calibrate the stochastic channel model in [161]. Based on the ML algorithm, the work in [162] exploited spatial correlation to predict path loss. The implicit correlation between AoD and AoA was revealed using a neural network in [163]. The work

in [152] applied ML to calibrate an uplink/downlink MIMO channel based on a deep neural network. In [164], a hybrid ray-launching neural network technique for fast radio propagation prediction using a combination of ray-launching and neural networks was proposed.

2) AI/ML ASSISTANCE IN HST SIGNAL PROCESSING

As mentioned in Section V-A, due to the complicated channel conditions, nonlinear electronic device behavior, and hybrid system architecture, the HST physical layer design generally involves multi-dimensional, non-convex, and nonlinear problems with complex and intractable solutions. In addition, the HST scenario involves delay-stringent applications that make the blockwise design highly suboptimal. Conventional signal processing procedures such as channel estimation and CSI feedback should be revisited because the imposed latency constraint might prevent the TX/RX from performing an accurate channel estimation. Therefore, an AI/ML-based algorithm is perfect for mimicking the performance of an intractable, nonlinear, single block and end-to-end function, and thus provides a rather good performance for the physical layer design. The work in [165] exhibits a deep reinforcement learning multi-agent power allocation algorithm to maximize the spectrum efficiency of a smart railway system. The authors of [166] proposed an ML algorithm to estimate the Doppler shift based on the value pattern of the reference signal RSRP. In [167], the decision on which direction to measure in the HST beam searching procedure is formulated into a sequential and selection problem that can be solved by the multi-armed bandit algorithm in reinforcement learning. A deep learning HST channel estimation with both offline training and an online channel prediction network with a convolutional neural network and a long short-term memory network was designed in [168]. The work in [169] proposed a deep learning algorithm to predict coordinated beamforming in a high-mobility mmWave communication system. Beamforming vectors for multiple BSs that jointly serve a UE are directly predicted from the signals received at the distributed BSs during the uplink training phase.

3) AI/ML ASSISTANCE IN HST DISTRIBUTED COOPERATION

Distributed cooperation in HST is another use case in which AI/ML assistance plays a key role. This refers to the case where multiple agents aim to cooperate to achieve a common goal based on different information. Coordinated beamforming, interference coordination, and limited-rate CoMP for multiple mobile relays or RRHs are typical distributed cooperation use cases. Distributed cooperation problems are famous because they are notoriously difficult to tackle [151], and the local input data at each agent are typically noisy, with the noise level possibly being different from agent to agent. The communication capability for information exchange between agents is often limited in terms of rate and/or latency. Each agent makes decision under partial and discrepant information in a cooperative manner. The problem remains open because of all the features mentioned above, and no good approximate solution is available. The distributed cooperation problem has also been extensively studied in AI and ML societies. In multi-agent reinforcement learning for coordination, they try to tackle the team coordination problem, where each agent is responsible for a portion of the problem, and the decisions of one agent will affect the performance or solution of other agents. In multi-agent reinforcement learning for n-player cooperative repeat games, as shown in Fig. 18, agents interact in a limited resource environment and select actions that maximize a single reward. Each joint action consists of a player action associated with a single reward function. The decision problem is cooperative given the fact that there is a single reward function reflecting the utility assessment of all agents.

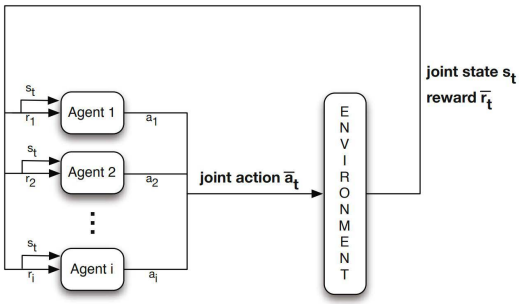

FIGURE 18. Multi-agent acting in the same environment [170].

These problems have been extensively studied using multi-agent reinforcement learning. Techniques such as parallel multiple-agent policy updates [171], swarm-based techniques [172], and learning state-space division among agents [173] have been proposed. In the HST scenario, a recent work in [174] established a Bayesian-adaptive partially observable Markov decision process and applied multi-agent Bayesian reinforcement learning for joint spectrum management of BS groups to tackle the problem of spectrum volatility due to high mobility and frequent handover.

4) AI/ML MODEL DISTRIBUTION AND TRANSFER IN HST

The accuracy of AI and ML algorithms depends on whether the data used to train the neural network are drawn from the same or similar distribution as the true application. Because dozens of sub-scenarios exist in HST and each of them has very distinct propagation conditions, to allow them to work properly during the journey of a train, AI/ML model update should be anticipated, and appropriate model distribution and transfer should be managed in the HST scenario. Indeed, in 3GPP, 5G system support for AI/ML model distribution and transfer has been studied for release 18 [175]. In the technical report, at least three types of AI/ML operations were supported in 5G:

- AI/ML operation splitting between AI/ML endpoints.
- AI/ML model/data distribution and sharing over 5G system.
- Distributed/Federated Learning over 5G system.

FIGURE 19. Operator cloud for model management [175].

A specific use case called AI model management as a Service [175] is illustrated in 3GPP. As is shown in Fig. 19, the 3rd party entities make use of AI models to support different kinds of services. However, considering the large size of AI models, strict downloading time, and UE capability, it is appropriate for a 3rd party to authorize professional companies to manage their AI models rather than doing the same thing locally by themselves. In AI model management, a 3rd party can invoke capabilities exposed by the 5G system to upload, download, update, delete, store and monitor AI models. AI models that are suitable for the situation are delivered to the UE over time. As the 5G system may collect communication data and user experience, it may perform a data analytic function for user experience, which can generate analysis results to help the operator's cloud train and improve AI models for the 3rd party.

In the HST scenario, owing to its high mobility and highly non-stationary nature, it is crucial to maintain a continuous approach for current AI model adaptation as well as AI model anticipation in the upcoming time and location. Current AI model adaptation refers to the procedure to adjust the model trained from offline data with a limited amount of online data to fight against model mismatches. AI model anticipation is the procedure used to decide the right moment to invoke model management and guarantee seamless model transfer during the transition. To the best of our knowledge, AI model management for HST has not yet been investigated. However, this is an important problem that can have a significant impact on the efficiency and reliability of AI/ML-aided algorithms and therefore should be addressed in the future.

VI. CONCLUSION

This tutorial seeks to provide a comprehensive view of the challenges and problems in HST communication, as well as physical layer enhancement technologies that contribute to the suppression of such problems.

In Section I-A, this tutorial began with an introduction to the challenges and difficulties linked to the harsh communication environment, dedicated railway applications, and frequency scarcity due to HST regulation.

In Section II, we review different technologies, both conventional and emerging, that can enhance the physical layer performance for HST. The MIMO family technologies are presented in Section II. Conventional single-user, multi-user MIMO beamforming, advanced multi-TRP, multi-cell MIMO cooperation, and relay assistance in HST were elaborated.

In Section III, nascent RIS technology and its application to HST are investigated. The capabilities of the RIS in beamforming, interference management, channel estimation, throughput and energy efficiency optimization, Doppler compensation, network deployment optimization, penetration loss reduction, and location and sensing were analyzed in detail.

The dedicated design of the control channel, reference signal, waveform, and numerology for mobility scenarios such as HST are presented in Section IV. Dedicated designs for DM-RS, PT-RS, and TRS to target high mobility, Doppler, and frequency were revealed. Considerations of the waveform and numerology for the HST are also discussed.

Section V presents recent advances in AI and ML for the HST physical layer. Challenges for AI/ML assistance in HST are presented and several concrete case studies are introduced.

ACKNOWLEDGMENT

The authors gratefully acknowledge the constructive discussions with Dr. Cristina Ciochina.

REFERENCES

[1] *Study on Scenarios and Requirements for Next Generation Access Technologies*, Standard TR38.913, Technical Specification Group Radio Access Network, 3rd Generation Partnership Project (3GPP), Tech. Rep., Jul. 2020.

[2] B. Ai, K. Guan, M. Rupp, T. Kurner, X. Cheng, X.-F. Yin, Q. Wang, G.-Y. Ma, Y. Li, L. Xiong, and J.-W. Ding, "Future railway services-oriented mobile communications network," *IEEE Commun. Mag.*, vol. 53, no. 10, pp. 78–85, Oct. 2015.

[3] J. Wu and P. Fan, "A survey on high mobility wireless communications: Challenges, opportunities and solutions," *IEEE Access*, vol. 4, pp. 450–476, 2016.

[4] K. Guan, B. Ai, B. Peng, D. He, G. Li, J. Yang, Z. Zhong, and T. Kurner, "Towards realistic high-speed train channels at 5G millimeter-wave band—Part I: Paradigm, significance analysis, and scenario reconstruction," *IEEE Trans. Veh. Technol.*, vol. 67, no. 10, pp. 9112–9128, Oct. 2018.

[5] K. Guan, B. Ai, B. Peng, D. He, G. Li, J. Yang, Z. Zhong, and T. Kurner, "Towards realistic high-speed train channels at 5G millimeter-wave band—Part II: Case study for paradigm implementation," *IEEE Trans. Veh. Technol.*, vol. 67, no. 10, pp. 9129–9144, Oct. 2018.

[6] J. Kim, M. Schmieder, M. Peter, H. Chung, S.-W. Choi, I. Kim, and Y. Han, "A comprehensive study on mmWave-based mobile hotspot network system for high-speed train communications," *IEEE Trans. Veh. Technol.*, vol. 68, no. 3, pp. 2087–2101, Mar. 2019.

[7] B. Ai, X. Cheng, T. Kürner, Z.-D. Zhong, K. Guan, R.-S. He, L. Xiong, D. W. Matolak, D. G. Michelson, and C. Briso-Rodriguez, "Challenges toward wireless communications for high-speed railway," *IEEE Trans. Intell. Transp. Syst.*, vol. 15, no. 5, pp. 2143–2158, Oct. 2014.

[8] J. Moreno, L. de Haro, C. Rodriguez, L. Cuellar, and J. M. Riera, "Keyhole estimation of an MIMO-OFDM train-to-wayside communication system on subway tunnels," *IEEE Antennas Wireless Propag. Lett.*, vol. 14, pp. 88–91, 2015.

[9] Y. Cocheril, M. Berbineau, P. Combeau, and Y. Pousset, "On the importance of the MIMO channel correlation in underground railway tunnels," *J. Commun.*, vol. 4, no. 4, pp. 224–231, May 2009.

[10] D. Seetharamdoo, R. Addaci, V. X. Pham, C. Chagny, K. Yang, J.-P. Ghys, and M. Berbineau, "Influence of railway environment on antenna performances at mm-wave frequencies," in *Proc. 11th Eur. Conf. Antennas Propag. (EUCAP)*, Mar. 2017, pp. 2899–2902.

[11] S. Dudoyer, V. Deniau, R. Adriano, M. N. B. Slimen, J. Rioult, B. Meyniel, and M. Berbineau, "Study of the susceptibility of the GSM-R communications face to the electromagnetic interferences of the rail environment," *IEEE Trans. Electromagn. Compat.*, vol. 54, no. 3, pp. 667–676, Jun. 2012.

[12] K. Hassan, R. Gautier, I. Dayoub, M. Berbineau, and E. Radoi, "Multiple-antenna-based blind spectrum sensing in the presence of impulsive noise," *IEEE Trans. Veh. Technol.*, vol. 63, no. 5, pp. 2248–2257, Jun. 2014.

[13] D. Seetharamdoo, R. Addaci, V. X. Pham, C. Chagny, K. Yang, J.-P. Ghys, and M. Berbineau, "Influence of railway environment on antenna performances at mm-wave frequencies," in *Proc. 11th Eur. Conf. Antennas Propag. (EUCAP)*, Mar. 2017, pp. 2899–2902.

[14] S. Sand, P. Unterhuber, D. B. Ahmed, F. D. P. Müller, A. Lehner, I. Rashdan, M. Schmidhammer, R. Karasek, B. Siebler, O. Heirich, C. Gentner, M. Walter, S. Kaiser, M. Ulmschneider, M. Schaab, L. Wientgens, and T. Strang, "Radio interference measurements for urban cooperative intelligent transportation systems," in *Proc. IEEE 94th Veh. Technol. Conf. (VTC-Fall)*, Sep. 2021, pp. 1–6.

[15] *White Paper: Security Against Electromagnetic Attacks, French Institute of Science and Technology for Transport, Development and Networks (IFSTTAR)*, Security of Railways Against Electromagnetic Attack (SECRET) Project Consortium, Villeneuve-d'Ascq, France, 2015.

[16] I. Lopez, M. Aguado, and C. Pinedo, "A step up in European rail traffic management systems: A seamless fail recovery scheme," *IEEE Veh. Technol. Mag.*, vol. 11, no. 2, pp. 52–59, Jun. 2016.

[17] D. Franco, M. Aguado, C. Pinedo, I. Lopez, I. Adin, and J. Mendizabal, "A contribution to safe railway operation: Evaluating the effect of electromagnetic disturbances on Balise-to-BTM communication in railway control signaling systems," *IEEE Veh. Technol. Mag.*, vol. 16, no. 2, pp. 104–112, Jun. 2021.

[18] A. Mohammadian and C. Tellambura, "Joint channel and phase noise estimation and data detection for GFDM," *IEEE Open J. Commun. Soc.*, vol. 2, pp. 915–933, 2021.

[19] *Future Railway Mobile Communication System; User Requirements Specification*, document FU-7100, International Union of Railways (UIC), Tech. Rep. Feb. 2020.

[20] *Future Railway Mobile Communication System; Use Cases*, document MG-7900, International Union of Railways (UIC), Tech. Rep., Feb. 2020.

[21] *Mobile Communication System for Railways*, Standard TS 22.289, Technical Specification Group Services and System Aspects; 3rd Generation Partnership Project (3GPP), Tech. Rep., Dec. 2019.

[22] *Rail Telecommunications (RT); Next Generation Communication System; Radio Performance Simulations and Evaluations in Rail Environment—Part 2: New Radio (NR)*, Standard TR 103 554-2, ETSI, Tech. Rep., Feb. 2021.

[23] *Commission Implementing Decision (EU) 2021/1730 of 28 September 2021 on the Harmonised Use of the Paired Frequency Bands 874.4–880.0 MHz and 919.4–925.0 MHz and of the Unpaired Frequency Band 1 900–1 910 MHz for Railway Mobile Radio*, European Commission, Off. J. Eur. Union, Brussels, Belgium, Sep. 2021.

[24] *5GRail Project Consortium, Deliverable D6.1, Scenarios for Rail and Road Communication System Coexistence, 5GRAIL Project, Grant no 951725*, Int. Union Railways, Paris, France, Jul. 2021.

[25] *5GRail Project Consortium, Deliverable D6.2, Implementation of the Selected Scenarios, Analysis and Conclusion, 5GRAIL Project, Grant no 951725*, Int. Union Railways, Paris, France, to be published.

[26] E. Telatar, "Capacity of multi-antenna Gaussian channels," *Eur. Trans. Telecommun.*, vol. 10, pp. 585–595, Nov. 1999.

[27] Y. Hu, W. Hong, and Z. H. Jiang, "A multibeam folded reflectarray antenna with wide coverage and integrated primary sources for millimeter-wave massive MIMO applications," *IEEE Trans. Antennas Propag.*, vol. 66, no. 12, pp. 6875–6882, Dec. 2018.

[28] M. Beccaria, A. Massaccesi, P. Pirinoli, and L. H. Manh, "Multibeam transmitarrays for 5G antenna systems," in *Proc. IEEE 7th Int. Conf. Commun. Electron. (ICCE)*, Jul. 2018, pp. 217–221.

[29] A. Aziz, F. Yang, S. Xu, and M. Li, "A low-profile quad-beam transmitarray," *IEEE Antennas Wireless Propag. Lett.*, vol. 19, no. 8, pp. 1340–1344, Aug. 2020.

[30] T. Pham, J. Weng, K. Pham, F. Gallée, and R. Sauleau, "V-band beam-switching transmitarray antenna for 5G MIMO channel sounding," in *Proc. Eur. Conf. Antennas Propag. (EuCAP)*, Mar. 2019, pp. 1–5.

[31] W. Guo, W. Zhang, P. Mu, F. Gao, and B. Yao, "Angle-domain Doppler pre-compensation for high-mobility OFDM uplink with massive ULA," in *Proc. GLOBECOM IEEE Global Commun. Conf.*, Dec. 2017, pp. 1–6.

[32] S. Typos, V. Kalokidou, S. Armour, A. Doufexi, E. Mellios, and A. Nix, "Codebook performance evaluation of mmWave in train communications," in *Proc. IEEE 91st Veh. Technol. Conf. (VTC-Spring)*, May 2020, pp. 1–6.

[33] J. Cao, D. Berkovskyy, D. Kong, F. Tila, E. Mellios, and A. Nix, "Optimization of multi-basestation codebook beamforming for mmWave connections to high speed trains," in *Proc. 2nd IEEE Middle East North Afr. Commun. Conf. (MENACOMM)*, Nov. 2019, pp. 1–6.

[34] X. Chen, J. Lu, and P. Fan, "Massive MIMO beam-forming for high speed train communication: Directivity vs beamwidth," 2017, *arXiv:1702.02121*.

[35] K. Hassan, M. Masarra, M. Zwingelstein, and I. Dayoub, "Channel estimation techniques for millimeter-wave communication systems: Achievements and challenges," *IEEE Open J. Commun. Soc.*, vol. 1, pp. 1336–1363, 2020.

[36] J. Sheng, Z. Tang, Q. Zhu, C. Wu, Y. Wang, and B. Ai, "An improved interference alignment algorithm with user mobility prediction for high-speed railway wireless communication networks," *IEEE Access*, vol. 8, pp. 80468–80479, 2020.

[37] Q. Peng and C. Wen, "Dispatch coordination between high-speed and conventional rail systems," *J. Modern Transp.*, vol. 19, no. 1, pp. 19–25, Mar. 2011.

[38] N. Feng, S. Lin, G. Zhu, S. Li, and H. Zhang, "Interference performance analysis of frequency reuse techniques for LTE-R systems," in *Proc. 21st Int. Conf. Intell. Transp. Syst. (ITSC)*, Nov. 2018, pp. 3415–3420.

[39] D. Gesbert, S. V. Hanly, H. Huang, S. S. Shitz, O. Simeone, and W. Yu, "Multi-cell MIMO cooperative networks: A new look at interference," *IEEE J. Sel. Areas Commun.*, vol. 28, no. 9, pp. 1380–1408, Sep. 2010.

[40] Y. Lu, K. Xiong, P. Fan, and Z. Zhong, "Optimal multicell coordinated beamforming for downlink high-speed railway communications," *IEEE Trans. Veh. Technol.*, vol. 66, no. 10, pp. 9603–9608, Oct. 2017.

[41] I. Zakia, "Coordinated beamforming for high-speed trains in multiple HAP networks," in *Proc. Telecommun. Syst. Services Appl. (TSSA)*, Oct. 2017, pp. 1–4.

[42] T. Zhou, G. Chen, C.-X. Wang, J. Zhang, L. Liu, and Y. Liang, "Performance analysis and power allocation of mixed-ADC multi-cell millimeter-wave massive MIMO systems with antenna selection," *Frontiers Inf. Technol. Electron. Eng.*, vol. 22, no. 4, pp. 571–585, Apr. 2021.

[43] W. Chen, I. Ahmad, and K. Chang, "Co-channel interference management using eICIC/FeICIC with coordinated scheduling for the coexistence of PS-LTE and LTE-R networks," *EURASIP J. Wireless Commun. Netw.*, vol. 2017, no. 1, pp. 1–14, 2017.

[44] G. Fodor, J. Vinogradova, P. Hammarberg, K. K. Nagalapur, Z. T. Qi, H. Do, R. Blasco, and M. U. Baig, "5G new radio for automotive, rail, and air transport," *IEEE Commun. Mag.*, vol. 59, no. 7, pp. 22–28, Jul. 2021.

[45] F. Hasegawa, A. Taira, H. Nishimoto, A. Okazaki, A. Okamura, G. Noh, B. Hui, J. Lee, and I. Kim, "3GPP standardization activities in relay based 5G high speed train scenarios for the SHF band," in *Proc. IEEE Conf. Standards Commun. Netw. (CSCN)*, Sep. 2017, pp. 126–131.

[46] J. D. O. Sanchez and J. I. Alonso, "A two-hop MIMO relay architecture using LTE and millimeter wave bands in high-speed trains," *IEEE Trans. Veh. Technol.*, vol. 68, no. 3, pp. 2052–2065, Mar. 2019.

[47] *Study on Scenarios and Requirements for New Radio Access Technology Physical Layer Aspects*, Standard TR38.802, Technical Specification Group Radio Access Network, 3rd Generation Partnership Project (3GPP), Tech. Rep., Sep. 2017.

[48] L. Tian, J. Li, Y. Huang, J. Shi, and J. Zhou, "Seamless dual-link handover scheme in broadband wireless communication systems for high-speed rail," *IEEE J. Sel. Areas Commun.*, vol. 30, no. 4, pp. 708–718, May 2012.

[49] *Evolved Universal Terrestrial Radio Access (E-UTRA); Study on Mobile Relay*, Standard TR36.836, Technical Specification Group Radio Access Network, 3rd Generation Partnership Project (3GPP), Tech. Rep., Jun. 2014.

[50] M. Iturralde, T. Kerdoncuff, T. Galezowski, and X. Lagrange, "Mobile relays for urban rail transportation systems," *Telecommun. Syst.*, vol. 76, no. 4, pp. 553–568, 2021.

[51] C.-X. Wang, A. Ghazal, B. Ai, Y. Liu, and P. Fan, "Channel measurements and models for high-speed train communication systems: A survey," *IEEE Commun. Surveys Tuts.*, vol. 18, no. 2, pp. 974–987, 2nd Quart., 2016.

[52] J. Zhang, H. Du, P. Zhang, J. Cheng, and L. Yang, "Performance analysis of 5G mobile relay systems for high-speed trains," *IEEE J. Sel. Areas Commun.*, vol. 38, no. 12, pp. 2760–2772, Dec. 2020.

[53] R. He, A. F. Molisch, Z. Zhong, B. Ai, J. Ding, R. Chen, and Z. Li, "Measurement based channel modeling with directional antennas for high-speed railways," in *Proc. IEEE Wireless Commun. Netw. Conf. (WCNC)*, Apr. 2013, pp. 2932–2936.

[54] R. He, Z. Zhong, B. Ai, G. Wang, J. Ding, and A. F. Molisch, "Measurements and analysis of propagation channels in high-speed railway viaducts," *IEEE Trans. Wireless Commun.*, vol. 12, no. 2, pp. 794–805, Feb. 2013.
[55] T. Zhou, C. Tao, L. Liu, and Z. Tan, "A semiempirical MIMO channel model in obstructed viaduct scenarios on high-speed railway," *Int. J. Antennas Propag.*, vol. 2014, pp. 1–10, Sep. 2014.
[56] B. Zhang, Z. Zhong, B. Ai, D. Yao, and R. He, "Measurements and modeling of cross-correlation property of shadow fading in high-speed railways," in *Proc. IEEE 80th Veh. Technol. Conf. (VTC-Fall)*, Sep. 2014, pp. 1–5.
[57] L. Liu, C. Tao, J. Qiu, H. Chen, L. Yu, W. Dong, and Y. Yuan, "Position-based modeling for wireless channel on high-speed railway under a viaduct at 2.35 GHz," *IEEE J. Sel. Areas Commun.*, vol. 30, no. 4, pp. 834–845, May 2012.
[58] J. Yang, B. Ai, S. Salous, K. Guan, D. He, G. Shi, and Z. Zhong, "An efficient MIMO channel model for LTE-R network in high-speed train environment," *IEEE Trans. Veh. Technol.*, vol. 68, no. 4, pp. 3189–3200, Apr. 2019.
[59] J. Lu, G. Zhu, and C. Briso-Rodriguez, "Fading characteristics in the railway terrain cuttings," in *Proc. IEEE 73rd Veh. Technol. Conf. (VTC Spring)*, May 2011, pp. 1–5.
[60] R. He, Z. Zhong, B. Ai, J. Ding, Y. Yang, and A. F. Molisch, "Short-term fading behavior in high-speed railway cutting scenario: Measurements, analysis, and statistical models," *IEEE Trans. Antennas Propag.*, vol. 61, no. 4, pp. 2209–2222, Apr. 2013.
[61] R. Sun, C. Tao, L. Liu, and Z. Tan, "Channel measurement and characterization for HSR U-shape groove scenarios at 2.35 GHz," in *Proc. IEEE 78th Veh. Technol. Conf. (VTC Fall)*, Sep. 2013, pp. 1–5.
[62] C. Briso-Rodriguez, J. M. Cruz, and J. I. Alonso, "Measurements and modeling of distributed antenna systems in railway tunnels," *IEEE Trans. Veh. Technol.*, vol. 56, no. 5, pp. 2870–2879, Sep. 2007.
[63] K. Guan, Z. Zhong, B. Ai, and T. Kurner, "Propagation measurements and analysis for train stations of high-speed railway at 930 MHz," *IEEE Trans. Veh. Technol.*, vol. 63, no. 8, pp. 3499–3516, Oct. 2014.
[64] G. Yue, D. Yu, L. Cheng, Q. Lv, Z. Luo, Q. Li, J. Luo, and X. He, "Millimeter-wave system for high-speed train communications between train and trackside: System design and channel measurements," *IEEE Trans. Veh. Technol.*, vol. 68, no. 12, pp. 11746–11761, Dec. 2019.
[65] P. T. Dat, A. Kanno, N. Yamamoto, and T. Kawanishi, "WDM RoF-MMW and linearly located distributed antenna system for future high-speed railway communications," *IEEE Commun. Mag.*, vol. 53, no. 10, pp. 86–94, Oct. 2015.
[66] S. Jaeckel, L. Raschkowski, K. Börner, and L. Thiele, "QuaDRiGa: A 3-D multi-cell channel model with time evolution for enabling virtual field trials," *IEEE Trans. Antennas Propag.*, vol. 62, no. 6, pp. 3242–3256, Jun. 2014.
[67] Y. Chang, M. Furukawa, H. Suzuki, and K. Fukawa, "Propagation analysis with ray tracing method for high speed trains environment at 60 GHz," in *Proc. IEEE 81st Veh. Technol. Conf. (VTC Spring)*, May 2015, pp. 1–5.
[68] K. Guan, G. Li, T. Kürner, A. F. Molisch, B. Peng, R. He, B. Hui, J. Kim, and Z. Zhong, "On millimeter wave and THz mobile radio channel for smart rail mobility," *IEEE Trans. Veh. Technol.*, vol. 66, no. 7, pp. 5658–5674, Jul. 2017.
[69] G. Li, B. Ai, K. Guan, R. He, Z. Zhong, B. Hui, and J. Kim, "Channel characterization for mobile hotspot network in subway tunnels at 30 GHz band," in *Proc. IEEE 83rd Veh. Technol. Conf. (VTC Spring)*, May 2016, pp. 1–5.
[70] G. Li, B. Ai, K. Guan, R. He, Z. Zhong, L. Tian, and J. Dou, "Path loss modeling and fading analysis for channels with various antenna setups in tunnels at 30 GHz band," in *Proc. 10th Eur. Conf. Antennas Propag. (EuCAP)*, Apr. 2016, pp. 1–5.
[71] X. Lin, B. Ai, D. He, K. Guan, Z. Zhong, L. Tian, and J. Dou, "Measurement based ray tracer calibration and channel analysis for high-speed railway viaduct scenario at 93.2 GHz," in *Proc. Antennas Propag. USNC/URSI Nat. Radio Sci. Meeting (AP-S/URSI)*, Jul. 2017, pp. 617–618.
[72] D. He, B. Ai, K. Guan, Z. Zhong, B. Hui, J. Kim, H. Chung, and I. Kim, "Channel measurement, simulation, and analysis for high-speed railway communications in 5G millimeter-wave band," *IEEE Trans. Intell. Transp. Syst.*, vol. 19, no. 10, pp. 3144–3158, Oct. 2018.
[73] J. Yang, B. Ai, K. Guan, D. He, X. Lin, B. Hui, J. Kim, and A. Hrovat, "A geometry-based stochastic channel model for the millimeter-wave band in a 3GPP high-speed train scenario," *IEEE Trans. Veh. Technol.*, vol. 67, no. 5, pp. 3853–3865, May 2018.
[74] W. Zeng, J. Zhang, K. P. Peppas, B. Ar, and Z. Zhong, "UAV-aided wireless information and power transmission for high-speed train communications," in *Proc. 21st Int. Conf. Intell. Transp. Syst. (ITSC)*, Nov. 2018, pp. 3409–3414.
[75] Q. Li and N. Gresset, "Multi-hop relaying in mmWave band for next generation train radio," in *Proc. IEEE 91st Veh. Technol. Conf. (VTC-Spring)*, May 2020, pp. 1–5.
[76] S. Scott, J. Leinonen, P. Pirinen, J. Vihriala, V. Van Phan, and M. Latva-Aho, "A cooperative moving relay node system deployment in a high speed train," in *Proc. IEEE 77th Veh. Technol. Conf. (VTC Spring)*, Jun. 2013, pp. 1–5.
[77] T. K. Vu, C.-F. Liu, M. Bennis, M. Debbah, and M. Latva-Aho, "Path selection and rate allocation in self-backhauled mmWave networks," in *Proc. IEEE Wireless Commun. Netw. Conf. (WCNC)*, Apr. 2018, pp. 1–6.
[78] D. Hu, J. Wu, and P. Fan, "Minimizing end-to-end delays in linear multi-hop networks," *IEEE Trans. Veh. Technol.*, vol. 65, no. 8, pp. 6487–6496, Aug. 2016.
[79] J. Yao, X. Zhou, Y. Liu, and S. Feng, "Secure transmission in linear multihop relaying networks," *IEEE Trans. Wireless Commun.*, vol. 17, no. 2, pp. 822–834, Feb. 2018.
[80] N. Abuzainab and C. Touati, "Multihop relaying in millimeter wave networks: A proportionally fair cooperative network formation game," in *Proc. IEEE 82nd Veh. Technol. Conf. (VTC-Fall)*, Sep. 2015, pp. 1–5.
[81] *Overview of 3GPP Release 10*, Standard 3rd Generation Partnership Project (3GPP), Tech. Rep., Jul. 2014.
[82] M. Polese, M. Giordani, T. Zugno, A. Roy, S. Goyal, D. Castor, and M. Zorzi, "Integrated access and backhaul in 5G mmWave networks: Potential and challenges," *IEEE Commun. Mag.*, vol. 58, no. 3, pp. 62–68, Mar. 2020.
[83] *Study on Integrated Access and Backhaul*, Standard TR38.874, Technical Specification Group Radio Access Network, 3rd Generation Partnership Project (3GPP), Tech. Rep., Dec. 2018.
[84] *IAB Enhancements for Rel-17*, Standard AT&T, RP-192709, 3rd Generation Partnership Project (3GPP), Tech. Rep., Dec. 2019.
[85] *Workplan for Rel-17 IAB*, Standard R1-2107364, Qualcomm Incorporated, Samsung, 3rd Generation Partnership Project (3GPP), Tech. Rep., Aug. 2021.
[86] *New WID on Mobile IAB*, Standard RP-213601, Qualcomm Incorporated, 3rd Generation Partnership Project (3GPP), Tech. Rep., Dec. 2021.
[87] *Study on Vehicle-Mounted Relays*, Standard TR22.839, Technical Specification Group Services and System Aspects, 3rd Generation Partnership Project (3GPP), Tech. Rep., Sep. 2021.
[88] *NG-RAN Architecture Description*, Standard TS38.401, Technical Specification Group Radio Access Network, 3rd Generation Partnership Project (3GPP), Tech. Rep., Oct. 2021.
[89] Y. Zhang, M. A. Kishk, and M.-S. Alouini, "A survey on integrated access and backhaul networks," 2021, *arXiv:2101.01286*.
[90] O. Teyeb, A. Muhammad, G. Mildh, E. Dahlman, F. Barac, and B. Makki, "Integrated access backhauled networks," in *Proc. IEEE 90th Veh. Technol. Conf. (VTC-Fall)*, Sep. 2019, pp. 1–5.
[91] C. Madapatha, B. Makki, C. Fang, O. Teyeb, E. Dahlman, M.-S. Alouini, and T. Svensson, "On integrated access and backhaul networks: Current status and potentials," *IEEE Open J. Commun. Soc.*, vol. 1, pp. 1374–1389, 2020.
[92] D. Gündüz, M. A. Khojastepour, A. Goldsmith, and H. V. Poor, "Multi-hop MIMO relay networks: Diversity-multiplexing trade-off analysis," *IEEE Trans. Wireless Commun.*, vol. 9, no. 5, pp. 1738–1747, May 2010.
[93] H. Q. Ngo and E. G. Larsson, "Linear multihop amplify-and-forward relay channels: Error exponent and optimal number of hops," *IEEE Trans. Wireless Commun.*, vol. 10, no. 11, pp. 3834–3842, Nov. 2011.
[94] Y. M. Khattabi and M. M. Matalgah, "Performance analysis of multiple-relay AF cooperative systems over Rayleigh time-selective fading channels with imperfect channel estimation," *IEEE Trans. Veh. Technol.*, vol. 65, no. 1, pp. 427–434, Jan. 2016.
[95] N. Varshney and P. Puri, "Performance analysis of decode-and-forward-based mixed MIMO-RF/FSO cooperative systems with source mobility and imperfect CSI," *J. Lightw. Technol.*, vol. 35, no. 11, pp. 2070–2077, Jun. 1, 2017.

[96] Q. Li, A. Charaf, N. Gresset, and H. Bonneville, "Radio resource management in next-generation railway system with heterogeneous multi-hop relaying deployment," in *Proc. Workshop Commun. Technol. Vehicles (Nets4Workshop)*, 2021, pp. 59–70.

[97] M. Choi, B. Yoon, D. Kim, and D. Sung, "IAB-based railway communication method for stable service provision," in *Proc. 12th Int. Conf. Ubiquitous Future Netw. (ICUFN)*, Aug. 2021, pp. 176–178.

[98] E. Basar, M. D. Renzo, J. De Rosny, M. Debbah, M. Alouini, and R. Zhang, "Wireless communications through reconfigurable intelligent surfaces," *IEEE Access*, vol. 7, pp. 116753–116773, 2019.

[99] C. Liaskos, S. Nie, A. Tsioliaridou, A. Pitsillides, S. Ioannidis, and I. Akyildiz, "A new wireless communication paradigm through software-controlled metasurfaces," *IEEE Commun. Mag.*, vol. 56, no. 9, pp. 162–169, Sep. 2018.

[100] E. Björnson, H. Wymeersch, B. Matthiesen, P. Popovski, L. Sanguinetti, and E. de Carvalho, "Reconfigurable intelligent surfaces: A signal processing perspective with wireless applications," 2021, *arXiv:2102.00742*.

[101] M. D. Renzo, M. Debbah, D. T. Phan-Huy, A. Zappone, M. S. Alouini, C. Yuen, V. Sciancalepore, G. C. Alexandropoulos, J. Hoydis, H. Gacanin, and J. D. Rosny, "Smart radio environments empowered by reconfigurable AI meta-surfaces: An idea whose time has come," *EURASIP J. Wireless Commun. Netw.*, vol. 2019, no. 1, pp. 1–20, May 2019.

[102] C. Huang, A. Zappone, G. C. Alexandropoulos, M. Debbah, and C. Yuen, "Reconfigurable intelligent surfaces for energy efficiency in wireless communication," *IEEE Trans. Wireless Commun.*, vol. 18, no. 8, pp. 4157–4170, Aug. 2019.

[103] E. Basar, "Reconfigurable intelligent surface-based index modulation: A new beyond MIMO paradigm for 6G," *IEEE Trans. Commun.*, vol. 68, no. 5, pp. 3187–3196, May 2020.

[104] D.-H. Kwon and S. A. Tretyakov, "Arbitrary beam control using passive lossless metasurfaces enabled by orthogonally polarized custom surface waves," *Phys. Rev. B, Condens. Matter*, vol. 97, no. 3, Jan. 2018, Art. no. 035439.

[105] Q. Wu and R. Zhang, "Towards smart and reconfigurable environment: Intelligent reflecting surface aided wireless network," *IEEE Commun. Mag.*, vol. 58, no. 1, pp. 106–112, Nov. 2019.

[106] E. Björnson, Ö. Özdogan, and E. G. Larsson, "Reconfigurable intelligent surfaces: Three myths and two critical questions," *IEEE Commun. Mag.*, vol. 58, no. 12, pp. 90–96, Dec. 2020.

[107] Q. Wu and R. Zhang, "Intelligent reflecting surface enhanced wireless network via joint active and passive beamforming," *IEEE Trans. Wireless Commun.*, vol. 18, no. 11, pp. 5394–5409, Nov. 2019.

[108] C. Huang, S. Hu, G. C. Alexandropoulos, A. Zappone, C. Yuen, R. Zhang, M. D. Renzo, and M. Debbah, "Holographic MIMO surfaces for 6G wireless networks: Opportunities, challenges, and trends," *IEEE Wireless Commun.*, vol. 27, no. 5, pp. 118–125, Oct. 2020.

[109] M. D. Renzo, K. Ntontin, J. Song, F. H. Danufane, X. Qian, F. Lazarakis, J. D. Rosny, D. T. Phan-Huy, O. Simeone, R. Zhang, and M. Debbah, "Reconfigurable intelligent surfaces vs. Relaying: Differences, similarities, and performance comparison," *IEEE Open J. Commun. Soc.*, vol. 1, pp. 798–807, 2020.

[110] C. Pan, H. Ren, K. Wang, M. Elkashlan, A. Nallanathan, J. Wang, and L. Hanzo, "Intelligent reflecting surface aided MIMO broadcasting for simultaneous wireless information and power transfer," *IEEE J. Sel. Areas Commun.*, vol. 38, no. 8, pp. 1719–1734, Aug. 2020.

[111] Z. Ma, Y. Wu, M. Xiao, G. Liu, and Z. Zhang, "Interference suppression for railway wireless communication systems: A reconfigurable intelligent surface approach," *IEEE Trans. Veh. Technol.*, vol. 70, no. 11, pp. 11593–11603, Nov. 2021.

[112] X. Wei, D. Shen, and L. Dai, "Channel estimation for RIS assisted wireless communications—Part I: Fundamentals, solutions, and future opportunities," *IEEE Commun. Lett.*, vol. 25, no. 5, pp. 1398–1402, May 2021.

[113] H. Liu, J. Zhang, Q. Wu, Y. Jin, Y. Chen, and B. Ai, "RIS-aided next-generation high-speed train communications: Challenges, solutions, and future directions," 2021, *arXiv:2103.09484*.

[114] M. Jian and Y. Zhao, "A modified off-grid SBL channel estimation and transmission strategy for RIS-assisted wireless communication systems," in *Proc. Int. Wireless Commun. Mobile Comput. (IWCMC)*, Jun. 2020, pp. 1848–1853.

[115] P. Wang, J. Fang, H. Duan, and H. Li, "Compressed channel estimation for intelligent reflecting surface-assisted millimeter wave systems," *IEEE Signal Process. Lett.*, vol. 27, pp. 905–909, 2020.

[116] J. Chen, Y.-C. Liang, H. V. Cheng, and W. Yu, "Channel estimation for reconfigurable intelligent surface aided multi-user MIMO systems," 2019, *arXiv:1912.03619*.

[117] S. Hu, F. Rusek, and O. Edfors, "Beyond massive MIMO: The potential of data transmission with large intelligent surfaces," *IEEE Trans. Signal Process.*, vol. 66, no. 10, pp. 2746–2758, May 2018.

[118] H. Guo, Y.-C. Liang, J. Chen, and E. G. Larsson, "Weighted sum-rate optimization for intelligent reflecting surface enhanced wireless networks," 2019, *arXiv:1905.07920*.

[119] E. C. Strinati, G. C. Alexandropoulos, V. Sciancalepore, M. D. Renzo, H. Wymeersch, D.-T. Phan-Huy, M. Crozzoli, R. D'Errico, E. D. Carvalho, P. Popovski, P. D. Lorenzo, L. Bastianelli, M. Belouar, J. E. Mascolo, G. Gradoni, S. Phang, G. Lerosey, and B. Denis, "Wireless environment as a service enabled by reconfigurable intelligent surfaces: The RISE-6G perspective," 2021, *arXiv:2104.06265*.

[120] B. Ai, A. F. Molisch, M. Rupp, and Z.-D. Zhong, "5G key technologies for smart railways," *Proc. IEEE*, vol. 108, no. 6, pp. 856–893, Jun. 2020.

[121] Y. Zhao, J. Zhang, and B. Ai, "Applications of reconfigurable intelligent surface in smart high speed train communications," 2021, *arXiv:2109.04354*.

[122] Q. Du, G. Wu, Q. Yu, and S. Li, "ICI mitigation by Doppler frequency shift estimation and pre-compensation in LTE-R systems," in *Proc. Int. Conf. Commun. China (ICCC)*, Aug. 2012, pp. 469–474.

[123] Y. Zhou, "Radio environment map based maximum a posteriori Doppler shift estimation for LTE-R," in *Proc. Int. Workshop High Mobility Wireless Commun.*, Nov. 2014, p. 5.

[124] B. Matthiesen, E. Bjornson, E. D. Carvalho, and P. Popovski, "Intelligent reflecting surface operation under predictable receiver mobility: A continuous time propagation model," *IEEE Wireless Commun. Lett.*, vol. 10, no. 2, pp. 216–220, Feb. 2021.

[125] L. Yang, Y. Yang, M. O. Hasna, and M.-S. Alouini, "Coverage, probability of SNR gain, and DOR analysis of RIS-aided communication systems," *IEEE Wireless Commun. Lett.*, vol. 9, no. 8, pp. 1268–1272, Aug. 2020.

[126] J. Zhang, E. Bjornson, M. Matthaiou, D. W. K. Ng, H. Yang, and D. J. Love, "Prospective multiple antenna technologies for beyond 5G," *IEEE J. Sel. Areas Commun.*, vol. 38, no. 8, pp. 1637–1660, Aug. 2020.

[127] S. Gong, X. Lu, D. T. Hoang, D. Niyato, L. Shu, D. I. Kim, and Y.-C. Liang, "Toward smart wireless communications via intelligent reflecting surfaces: A contemporary survey," *IEEE Commun. Surveys Tuts.*, vol. 22, no. 4, pp. 2283–2314, 4th Quart., 2020.

[128] H. Du, J. Zhang, J. Cheng, and B. Ai, "Millimeter wave communications with reconfigurable intelligent surfaces: Performance analysis and optimization," *IEEE Trans. Commun.*, vol. 69, no. 4, pp. 2752–2768, Apr. 2021.

[129] M. Gao, B. Ai, Y. Niu, Z. Han, and Z. Zhong, "IRS-assisted high-speed train communications: Outage probability minimization with statistical CSI," in *Proc. IEEE Int. Conf. Commun.*, Jun. 2021, pp. 1–6.

[130] N. Yu, P. Genevet, M. A. Kats, F. Aieta, J.-P. Tetienne, F. Capasso, and Z. Gaburro, "Light propagation with phase discontinuities: Generalized laws of reflection and refraction," *Science*, vol. 334, no. 6054, pp. 333–337, Oct. 2011.

[131] B. Duan, C. Li, and J. Xie, "Design of 5G wireless communications in the high-speed railway scenario," in *Proc. Veh. Technol. Conf. (VTC-Fall)*, Nov. 2020, pp. 1–6.

[132] C. E. O. Vargas and L. D. S. Mello, "Measurements of reflection and penetration loss of construction materials at 28 GHz and 38 GHz," in *Proc. IEEE-APS Topical Conf. Antennas Propag. Wireless Commun. (APWC)*, Sep. 2018, pp. 897–900.

[133] H. Wymeersch, J. He, B. Denis, A. Clemente, and M. Juntti, "Radio localization and mapping with reconfigurable intelligent surfaces: Challenges, opportunities, and research directions," *IEEE Veh. Technol. Mag.*, vol. 15, no. 4, pp. 52–61, Dec. 2020.

[134] G. Noh, B. Hui, J. Kim, H. S. Chung, and I. Kim, "DMRS design and evaluation for 3GPP 5G new radio in a high speed train scenario," in *Proc. GLOBECOM IEEE Global Commun. Conf.*, Dec. 2017, pp. 1–6.

[135] *Technical Specification Group Radio Access Network. Physical Channels and Modulation*, Standard (TS) 38.211, Sec. 7.4.1, 3rd Generation Partnership Project (3GPP)é, Technical Specification, Jun. 2021.

[136] M. H. C. Garcia, A. Molina-Galan, M. Boban, J. Gozalvez, B. Coll-Perales, T. Sahin, and A. Kousaridas, "A tutorial on 5G NR V2X communications," *IEEE Commun. Surveys Tuts.*, vol. 23, no. 3, pp. 1972–2026, 3rd Quart., 2021.

[137] *R1-1910532 PHY Layer Structure for NR Sidelink*, Standard 3GPP TSG-RAN WG1 Meeting #98bis, Ericsson, Stockholm, Sweden, 2019.
[138] W. C. Jakes, *Microwave Mobile Communications*. Hoboken, NJ, USA: Wiley, 1974.
[139] *RS Design for NR V2X Sidelink*, Standard R1-1912283 3GPP TSG-RAN WG1 Meeting #99, MERCE, 2019.
[140] *Technical Specification Group Radio Access Network; Study on Evaluation Methodology of New Vehicle-to-Everything (V2X) Use Cases for LTE and NR*, Standard (TR) 37.885, 3rd Generation Partnership Project (3GPP), Tech. Rep., Jun. 2019.
[141] E. Dahlman, S. Parkvall, and J. Skold, *5G NR: The Next Generation Wireless Access Technology*, 1st ed. New York, NY, USA: Academic, 2018.
[142] *PDSCH/PUSCH Enhancements for 52–71GHz Spectrum*, Standard R1-2108771 3GPP TSG-RAN WG1 Meeting #106bis-e, Huawei, Shenzhen, China, 2021.
[143] *PT-RS Enhancements for NR From 52.6GHz to 71GHz*, Standard R1-2109163 3GPP TSG-RAN WG1 Meeting #106bis-e, MERCE, 2021.
[144] *PDSCH/PUSCH Enhancements*, Standard R1-2109438 3GPP TSG-RAN WG1 Meeting #106bis-e, Ericsson, Stockholm, Sweden, 2021.
[145] J.-C. Sibel, C. Ciochina, and F. Hasegawa, "Evaluation of static sequence assisted DFT-spread-OFDM for 5G systems," in *Proc. IEEE 86th Veh. Technol. Conf. (VTC-Fall)*, Sep. 2017, pp. 1–5.
[146] M. Saideh, M. Berbineau, and I. Dayoub, "5G waveforms for railway," in *Proc. 15th Int. Conf. ITS Telecommun. (ITST)*, May 2017, pp. 1–5.
[147] Q. Zheng, F. Wang, X. Chen, Y. Liu, D. Miao, and Z. Zhao, "Comparison of 5G waveform candidates in high speed scenario," in *Proc. General Assembly Sci. Symp. Int. Union Radio Sci. (URSI GASS)*, Aug. 2017, pp. 1–4.
[148] F. Hasegawa, A. Taira, G. Noh, B. Hui, H. Nishimoto, A. Okazaki, A. Okamura, J. Lee, and I. Kim, "High-speed train communications standardization in 3GPP 5G NR," *IEEE Commun. Standards Mag.*, vol. 2, no. 1, pp. 44–52, Mar. 2018.
[149] *Discussion on the Necessity of Applying 60KHz SCS With ECP for High Speed Train Network*, Standard AT&T, 3rd Generation Partnership Project (3GPP), Tech. Rep., Mar. 2018.
[150] T. J. O'Shea and J. Hoydis, "An introduction to deep learning for the physical layer," *IEEE Trans. Cogn. Commun. Netw.*, vol. 3, no. 4, pp. 563–575, Oct. 2017.
[151] D. Gunduz, P. de Kerret, N. Sidiroupoulos, D. Gesbert, C. Murthy, and M. van der Schaar, "Machine learning in the air," *IEEE J. Sel. Areas Commun.*, vol. 37, no. 10, pp. 2184–2199, Oct. 2019.
[152] H. Huang, S. Guo, G. Gui, Z. Yang, J. Zhang, H. Sari, and F. Adachi, "Deep learning for physical-layer 5G wireless techniques: Opportunities, challenges and solutions," *IEEE Wireless Commun.*, vol. 27, no. 1, pp. 214–222, Feb. 2020.
[153] Z. Qin, H. Ye, G. Y. Li, and B. H. F. Juang, "Deep learning in physical layer communications," *IEEE Wireless Commun.*, vol. 26, no. 2, pp. 93–99, Mar. 2019.
[154] T. Wang, C.-K. Wen, H. Wang, F. Gao, T. Jiang, and S. Jin, "Deep learning for wireless physical layer: Opportunities and challenges," *China Commun.*, vol. 14, no. 11, pp. 92–111, 2017.
[155] H. He, S. Jin, C. Wen, F. Gao, G. Y. Li, and Z. Xu, "Model-driven deep learning for physical layer communications," *IEEE Wireless Commun.*, vol. 26, no. 5, pp. 77–83, Oct. 2019.
[156] A. Goldsmith, "Joint source/channel coding for wireless channels," in *Proc. IEEE 45th Veh. Technol. Conf Countdown Wireless 21st Century*, Jul. 1995, pp. 614–618.
[157] E. Zehavi, "8-PSK trellis codes for a Rayleigh channel," *IEEE Trans. Commun.*, vol. 40, no. 5, pp. 873–884, May 1992.
[158] M. Yin, K. Li, and X. Cheng, "A review on artificial intelligence in high-speed rail," *Transp. Saf. Environ.*, vol. 2, no. 4, pp. 247–259, Nov. 2020.
[159] K. Guan, H. Yi, D. He, B. Ai, and Z. Zhong, "Towards 6G: Paradigm of realistic terahertz channel modeling," *China Commun.*, vol. 18, no. 5, pp. 1–18, May 2021.
[160] Y. Chen, Y. Li, C. Han, Z. Yu, and G. Wang, "Channel measurement and ray-tracing-statistical hybrid modeling for low-terahertz indoor communications," 2021, *arXiv:2101.12436*.
[161] R. Adeogun, "Calibration of stochastic radio propagation models using machine learning," *IEEE Antennas Wireless Propag. Lett.*, vol. 18, no. 12, pp. 2538–2542, Dec. 2019.
[162] J. Thrane, D. Zibar, and H. L. Christiansen, "Model-aided deep learning method for path loss prediction in mobile communication systems at 2.6 GHz," *IEEE Access*, vol. 8, pp. 7925–7936, 2020.
[163] S. Navabi, C. Wang, O. Y. Bursalioglu, and H. Papadopoulos, "Predicting wireless channel features using neural networks," in *Proc. IEEE Int. Conf. Commun. (ICC)*, May 2018, pp. 1–6.
[164] L. Azpilicueta, M. Rawat, K. Rawat, F. Ghannouchi, and F. Falcone, "A ray launching-neural network approach for radio wave propagation analysis in complex indoor environments," *IEEE Trans. Antennas Propag.*, vol. 62, no. 5, pp. 2777–2786, May 2014.
[165] J. Xu and B. Ai, "Artificial intelligence empowered power allocation for smart railway," *IEEE Commun. Mag.*, vol. 59, no. 2, pp. 28–33, Feb. 2021.
[166] T. Kim, K. Ko, I. Hwang, D. Hong, S. Choi, and H. Wang, "RSRP-based Doppler shift estimator using machine learning in high-speed train systems," *IEEE Trans. Veh. Technol.*, vol. 70, no. 1, pp. 371–380, Jan. 2021.
[167] J.-B. Wang, M. Cheng, J.-Y. Wang, M. Lin, Y. Wu, H. Zhu, and J. Wang, "Bandit inspired beam searching scheme for mmWave high-speed train communications," 2018, *arXiv:1810.06150*.
[168] Y. Liao, Y. Hua, X. Dai, H. Yao, and X. Yang, "ChanEstNet: A deep learning based channel estimation for high-speed scenarios," in *Proc. IEEE Int. Conf. Commun. (ICC)*, May 2019, pp. 1–6.
[169] A. Alkhateeb, S. Alex, P. Varkey, Y. Li, Q. Qu, and D. Tujkovic, "Deep learning coordinated beamforming for highly-mobile millimeter wave systems," *IEEE Access*, vol. 6, pp. 37328–37348, 2018.
[170] A. Nowé, P. Vrancx, and Y.-M. D. Hauwere, "Game theory and multi-agent reinforcement learning," in *Reinforcement Learning*. Berlin, Germany: Springer, 2012, pp. 441–470.
[171] C. E. Mariano and E. F. Morales, "DQL: A new updating strategy for reinforcement learning based on Q-learning," in *Proc. Eur. Conf. Mach. Learn. Princ. Pract. Knowl. Discovery Databases (ECML PKDD)*, 2001, pp. 324–335.
[172] M. Dorigo, M. Birattari, and T. Stutzle, "Ant colony optimization," *IEEE Comput. Intell. Mag.*, vol. 1, no. 4, pp. 28–39, Nov. 2006.
[173] K. Steenhaut, A. Nowé, M. Fakir, and E. Dirkx, "Towards a hardware implementation of reinforcement learning for call admission control in networks for integrated services," in *Proc. Int. Workshop Appl. Neural Netw. Telecommun. (IWANNT)*, 1997, pp. 63–70.
[174] C. Wu, C. Wang, J. Sheng, and Y. Wang, "Cooperative learning for spectrum management in railway cognitive radio network," *IEEE Trans. Veh. Technol.*, vol. 68, no. 6, pp. 5809–5819, Jun. 2019.
[175] *Study on Traffic Characteristics and Performance Requirements for AI/ML Model Transfer in 5GS*, Standard TR22.874 Technical Specification Group Services and System Aspects, 3rd Generation Partnership Project (3GPP), Tech. Rep., Sep. 2021.

QIANRUI LI (Member, IEEE) received the B.Sc. degree in information engineering from Shanghai Jiao Tong University, Shanghai, China, in 2010, and the M.Eng. and Ph.D. degrees in electronics and communications from Télécom ParisTech, France, in 2012 and 2016, respectively. He is currently a Senior Researcher and a 3GPP RAN1 Delegate with Mitsubishi Electric Research and Development Centre Europe, Rennes, France. His research interests include signal processing, AI/ML assisted communication, physical layer design for 5G and beyond including cooperative transmission, massive MIMO, millimeter-wave communications, and vertical domain applications.

JEAN-CHRISTOPHE SIBEL received the engineering degree in signal processing and communications from ENSEA, Cergy-Pontoise, France, and the master's degree in intelligent communicating systems and the Ph.D. degree in science of technology of information and communications from the University of Cergy-Pontoise, in 2009 and 2013, respectively. He worked as a Postdoctoral Researcher with IETR, INSA of Rennes, on channel coding for DVB-S2; and with the CitiLab, INSA of Lyon, France, on wireless networks. He is currently a Researcher with Mitsubishi Electric Research and Development Centre Europe, Rennes. His research interests include signal processing and physical layer design for 5G and beyond, including cooperative transmission, millimeter-wave communications, and vertical domain applications.

MARION BERBINEAU (Member, IEEE) received the engineering degree in informatics, electronics, and automatics from Polytech Lille former EUDIL, in 1986, and the Ph.D. degree in electronics from the University of Lille, France, in 1989. She has been the Research Director with Université Gustave Eiffel (previously Ifsttar and Inrets), since 2000. She was the Director of the Leost laboratory, from 2000 to 2013; and then the Deputy Director of the COSYS Department, from 2013 to 2017. In addition to research activities and supervision of Ph.D. students, she coordinates railway research with Université Gustave Eiffel. She is the Vice-Chairperson of the European Railway Research Network of Excellence (EURNEX). Her current interests include wireless communications for connected and automatic vehicles (trains and cars) and, in particular, radio propagation, channel characterization, modeling, MCM, MIMO, millimetric waves, ITS-G5, GSM-R, LTE, and 5G NR. She has been participating in several European and national research projects, since 1990. She is currently the Project Leader of the mmW4Rail (mm Wave for Railway) Project in the framework of the National Research Agency. She is involved in several other projects at the European level (X2RAIL3, X2RAIL4, X2RAIL5, 5GRAIL, and INDID). She is on the reserve list of the Scientific Council of the Shift2Rail Joint Undertaking.

IYAD DAYOUB (Senior Member, IEEE) received the M.Sc. degree from the National Polytechnic Institute of Lorraine (INPL), in 1997, and the Ph.D. degree from the Valenciennes University/Institute of Electronics, Microelectronics and Nanotechnology (IEMN), in 2001. He is currently a Full Professor of communications engineering with Université Polytechnique Hauts-de-France (UPHF) and the National Institute of Applied Sciences/Hauts-de-France (INSA-H-d-F). He has worked as a Systems Engineer with Siemens, Damascus, Syria, from 1993 to 1995; and as a Researcher with Alcatel Business Systems, Colombes, Paris, from 1999 to 2000. He was a member of the National Council of Universities (CNU), France, from 2007 to 2014, in the area of electrical engineering, electronics, photonics and systems; and an Adjunct Professor with Concordia University, Montreal, from 2010 to 2014. His current research activities are developed at the IEMN (CNRS UMR 8520), where he is the Head of the Digital Communications Group (COMNUM). He is a member of several international conference advisory committees, technical program committees, and organization committees such as VTC, GLOBECOM, ICC, PIMRC, and WWC. He was the recipient of several awards, including the Excellence in Research Award (French Ministerial); and the Outstanding IEEE Publication Award, in 2018.

FRANÇOIS GALLÉE received the Ph.D. degree in electronics from the University of Brest, Brest, France, in 2001. From 2001 to 2007, he was a Research Engineer with ANTENNESSA. His main activities were antenna design and the development of a measurement setup for the assessment of the specific absorption rate (SAR) of wireless devices. Since 2007, he has been an Associate Professor with the Microwave Department IMT Atlantique, Brest. His research activities are lead in the CNRS Laboratory "Information and Communication Science and Technology" (Lab-STICC). He is responsible for the research team "RF devices." His research interests include antenna design for microwave and millimeter-wave applications, wireless communication in harsh environments, and RFID applications. About the topic "RF exposition," he has expertise in the design of equipment for the measurement of electromagnetic field and in the protocol measurement.

HERVÉ BONNEVILLE received the degree from the University of Paris XI, in 1987. He worked in telecommunication area and embedded real-time systems for Sagem, Transpac, and Thomson before joining Mitsubishi Electric Research and Development Centre Europe, in 1999. He participated in the conception and design of the MERCE HiperLAN/2 prototype, has been involved in the European projects IST-PULSER and ARTIS4G; and in the French project SYSTUF on radio systems design for urban rail control signaling. He has actively participated in IEEE 802.11n standardization and has contributed to 3GPP LTE/5G architecture standardization (RAN3, SA2), since 2006; and ETSI TC-RT, since 2016. His research interests include layers 2 and 3 of communication stacks, more specifically for wireless communications in the context of high QoS requirements and extend to networks architecture for radio access systems. He is currently working on QoS and mobility aspects for railway communications and architecture for 5G systems.